1955

Structure of molybdenum films deposited on single crystals of silver and rocksalt

Morris Mauss Christensen
Iowa State College

NOTE TO USERS

STRUCTURE OF MOLYBDENUM FILMS DEPOSITED ON SINGLE CRYSTALS OF SILVER AND ROCKSALT

by

Morris Mauss Christensen

A Dissertation Submitted to the
Graduate Faculty in Partial Fulfillment of
the Requirements for the Degree of
DOCTOR OF PHILOSOPHY

Major Subject: Electrical Engineering

Approved:

Signature was redacted for privacy.

In Charge of Major Work

Signature was redacted for privacy.

Head of Major Department

Signature was redacted for privacy.

Dean of Graduate School

Iowa State College

1955

TABLE OF CONTENTS

I. INTRODUCTION

Three years after DeBroglie (1) announced the wave nature of matter, Davisson and Germer (2) observed that a low-energy electron beam was preferentially scattered from the surface of a single crystal of nickel. Shortly afterwards Thomson (3) published the results of experiments on the diffraction of fast electrons by thin films of aluminum and gold. The next progress was reported by Nishikawa and Kikuchi (4) who obtained single-crystal reflection patterns while working with mica, calcite, quartz, topaz, and zinc blende. Since these experiments in the late 1920's, the method of electron diffraction has been extensively applied to the study of thin films and the structure of metallic surfaces.

The particular advantage of the use of fast electrons for the study of surface layers is due to the efficiency of scattering of electrons by matter, whence films only a few angstroms in thickness will give strong diffraction patterns (5). Metallic films thin enough to give a pattern by transmission of the electron beam have been prepared by condensation from the vapor state on fine gauze or on a substrate such as collodion or rock salt (6, 7). Specimens which are opaque to electrons having energies of 40 to 50 KV, or are not readily removed from the base material without undergoing some change are studied by the reflection method at nearly grazing incidence. In this case, coherent scattering is due to the electrons penetrating

small crystalline projections above the mean level of the surface (8).

In general, diffraction effects by either the transmission or the reflection methods are observed when the Bragg law is satisfied, i.e., when $\lambda = 2d \sin \theta$. The geometrical meaning of this relation is shown in Fig. 2. Here λ is the DeBroglie wave length of the incident electrons, d the spacing between successive identical planes of atoms in the crystal, and θ the angle between the electron beam and these atomic planes. Bragg (9) showed that this relation was equivalent to the three Laue conditions which, for the angles θ occurring in electron diffraction patterns, can be represented in a plane (the photographic plate) by a system of horizontal lines, vertical lines, and circles (10). A row of equally spaced atoms irradiated by an electron beam will give diffraction maxima along a series of cones with the atom-row as axis. A three-dimensional array of lattice points (atoms) gives rise to diffraction-cones which intersect the photographic plate in the lines and circles referred to above. When the system of lines and circles intersect in a point, a diffraction spot is observed; the diffracted beam being along the line of intersection of the three diffraction cones.

Now reflection patterns are observed which show Laue 'spots' of various shapes and intensities from broad diffuse lines to well defined reflections, either spots or rings. The electron beam is about 10^6 A.U. in width and hence covers many thousands of atoms so that the cone of reinforcement due to the lattice rows perpendicular to the beam and lying in the crystal surface will generally be sharp. The lines of reinforcement due to lattice rows normal to both the beam and the

surface form broad bands because of the limited depth of penetration of electrons at grazing incidence, with the result that a small number of atoms is available for coherent scattering. Depending upon the submicroscopic roughness of the crystal surface, the third lattice row parallel to the beam gives circular bands which may be very broad or relatively sharp.

To these effects on the diffraction pattern, associated with the relaxation of the Laue conditions for the various zones, must be added the effect of slight distortion in the crystal. A perfect crystal will reflect only over a range of a few seconds of arc in the Bragg angle. However most crystals have a mosaic structure in which different parts of the lattice are not quite parallel to each other. Hence each set of equivalent planes reflect over a range of several minutes (11). In terms of the reciprocal lattice, this type of distortion causes extension of the reciprocal lattice 'points' so that the sphere of reflection makes contact with each 'point' over a finite angle.

Mention has been made of the effect of surface roughness on the diffraction pattern. A metal surface rubbed with a fine-grained abrasive will give specular reflection for at least some incidence angle. French (12) studied the structure of mechanically polished metal surfaces by 'reflection' of electrons. He observed a pattern of diffuse haloes which was interpreted by him as being due to an amorphous or liquid-like polish layer, called the Beilby layer. However in 1935 Kirchner (13) found that exactly similar patterns were obtained with electrons at grazing incidence on the surface of evaporated gold films,

while transmission patterns of the same specimen gave sharp characteristic rings. He concluded that polishing merely levelled the surface so that any minute crystallites project above the surrounding areas, giving a diffraction pattern characteristic of small grain size (14). It is generally agreed, however, that mechanical polishing produces a disturbed layer of metal at the surface (15) which can best be removed by electrolytic polishing. This method of polishing metallic specimens was used in the present investigation.

It is not unusual for thin layers of metals condensed from the vapor in high vacuum to develop a preferred orientation with one type of crystal plane parallel to the surface of the substrate. Thus, Lassen and Brück (16) found that thin films of silver (a = 4.08 A.U.) deposited on the heat-treated (100) face of rock salt (a = 5.68 A.U.) followed the orientation of the rock salt, with a line of atoms in the metal parallel to a line of atoms in the salt. Above a critical temperature, nickel, gold, and platinum have been found to orient with their (100) and (111) planes parallel to the cube face of rock salt (17). Rhodin (18) examined the structure of thick deposits of aluminum on the cleavage face of alkali halides and found that orientation depended on the temperature and on the supporting crystal. Oriented overgrowth or epitaxy was observed by Schulz (19) using electron diffraction to study thin films of alkali halides on the cleaved crystals of other alkali halides. These experiments have yielded information on such important problems as the influence of temperature and thickness of the deposits on orientation and the mechanism of

crystal growth.

Closely related to the present problem, Shirai (20, 21) reported that molybdenum evaporated on to the (100) cleavage surface of rock salt assumes random orientation at room temperature but takes up preferred orientations when the rock salt is heated above a certain critical temperature during deposition.

The purpose of the present problem is to investigate the orientation of molybdenum crystals in a thin film that has been prepared by vacuum evaporation on the (100) face of silver. Special consideration is given to the orienting, cutting, and polishing of the silver crystal prior to evaporation of the molybdenum film.

II. APPARATUS AND EXPERIMENTAL PROCEDURE

The experimental procedures which were adopted for this investigation can be divided into four general groups: (A) orientation of the silver crystal, (B) cutting and polishing single crystals of silver and rocksalt, (C) preparation of a thin molybdenum film, and (D) determination of the structure of the molybdenum film as deposited on a silver crystal.

The techniques by which these four operations were accomplished are discussed separately and a complete description of each is given.

A. Orientation of Silver Crystal

A large single crystal of silver was obtained from Professor A. T. Gwathmey of the Virginia Institute for Scientific Research. The crystal as received was in the form of a cylinder approximately 5/8 inch in diameter and 6 inches in length and was pointed at one end. It was prepared from 99.99 per cent pure silver according to the Virginia Institute. Several glints could be observed around the circumference by rotating the crystal about the axis of the cylinder.

The problem of orienting such a large crystal specimen is better understood when one considers the method of growing metallic single crystals. The method (22) consists essentially of lowering slowly the

molten metal out of a furnace maintained at a temperature slightly above the melting point of the metal. A graphite rod which has been properly drilled to form a point at one end may be used as a crucible. The metal thus takes the form of a rod or cylinder pointed at the lower end so that one seed crystal forms at the tip as it passes out of the melting zone of the furnace. Then as the melt is lowered slowly, all of the metal solidifies on this nucleus to form one continuous crystal.

Growth of crystals in the solid state by the method outlined above yields a single-crystal structure as distinguished from a polycrystalline metal in which the individual crystallites are randomly oriented. The lattice orientation of the bulk crystal however is fixed by the orientation of the seed or 'nucleus'. As the seed may assume any orientation, the cylinder axis of the crystal will not usually be established as a principal crystallographic axis also. It is therefore essential to determine the orientation of the large crystal in order that the specimen may be cut parallel to net-planes of low, rational Miller indices.

One of the most accurate and convenient methods of determining the orientation of a single crystal is the back-reflection Laue method (23). The basic principle of the method is illustrated in Fig. 1. A beam of white X-radiation, I, passes perpendicularly through a hole in the photographic film holder M, is incident upon the crystal plane C, and is diffracted back to the film along R. Each important atomic plane selects the correct wave length to give

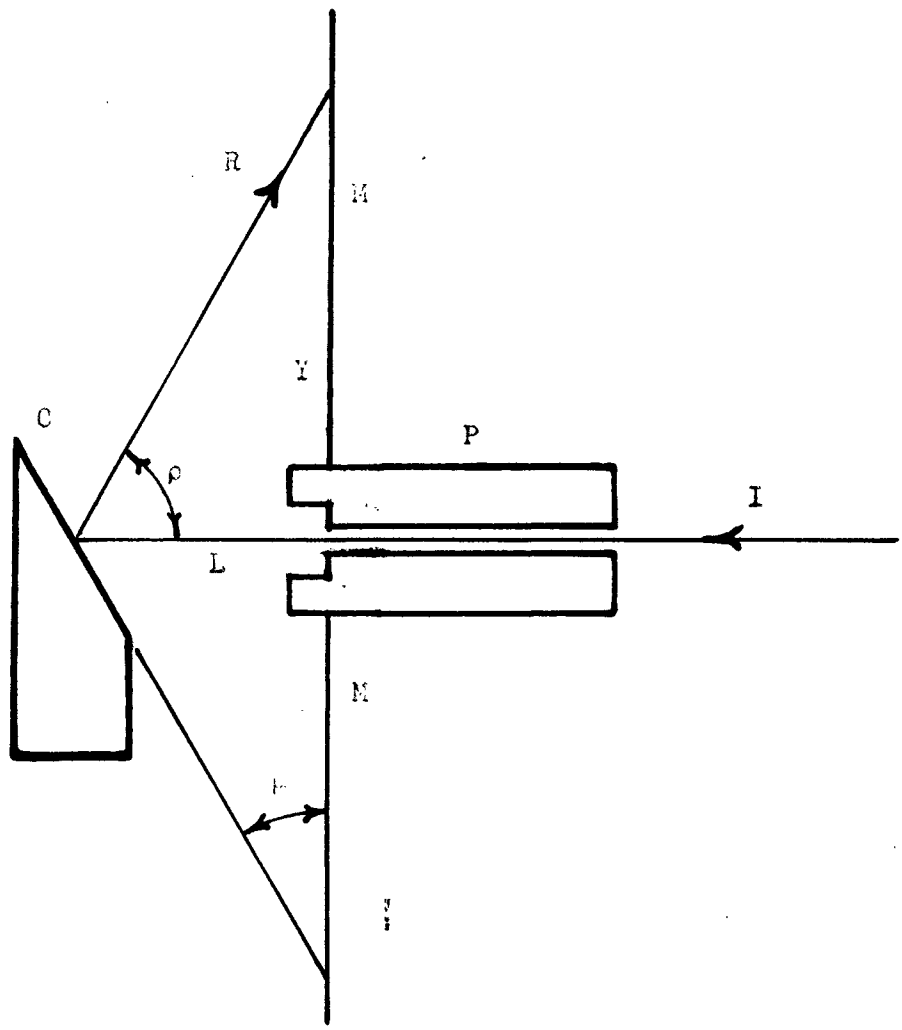

Fig. 1 - Schematic Diagram of Back Reflection Laue Photograph Showing the Incident Beam I and the Reflected Beam R at the Crystal Plane C.

a strong diffraction spot according to the Bragg equation

$$\lambda = 2d \sin \theta$$

shown geometrically in Fig. 2. When a given crystal plane is in position to reflect, a definite relationship exists between the angles in Fig. 1. Thus, for the conditions shown

$$\rho = 2\mu$$

and

$$Y = L \tan 2\mu.$$

The apparatus used for obtaining the X-ray diffraction patterns consisted of a back reflection camera built by the General Electric Company and modified for these experiments. The essential elements of the camera include a pin-hole system P, Fig. 1, lead cassette M for securing the film in position, and a goniometer mounted on grooved guides for adjusting the distance from the film to the crystal C. A pair of steel wires mounted on the cassette served as cross-hairs for orienting the diffraction pattern. Lead shields enclose the apparatus to provide protection to the operator from secondary radiation.

Most X-ray goniometers are designed for use with minute single crystals that can be mounted on a small glass fibre. However the rotations that are possible with the conventional goniometer are also desirable for orienting a massive crystal of the type being studied. A special mounting was therefore constructed by which the silver

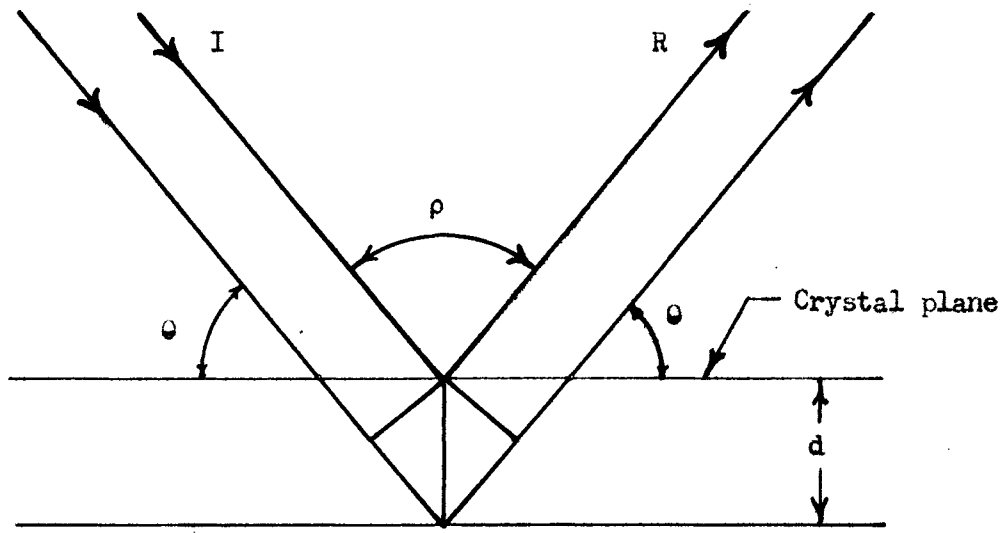

Fig. 2 - Geometrical Relations Among I, R and the Crystal Plane C when Bragg's Law is Satisfied.

crystal could be held securely in position, while at the same time its azimuth angle with respect to a fixed reference could be read on a horizontal graduated circle.

Another modification consisted of gaging the crystal-to-film distance. As stated above, the goniometer mounting permitted adjustment of the crystal-to-film distance; for reasons which will appear presently, a distance of 3 centimeters was used in these experiments. The method employed here for gaging this separation was as follows: A gage consisting of two small concentric cylinders was designed such that the outer cylinder could be fitted into the center hole of the film holder M, Fig. 1. The inner cylinder was set to give a separation of 3 centimeters between the film and the point at which the X-ray beam strikes the specimen. By means of a set-screw this inner cylinder could then be fixed at the 3 centimeter setting.

Let us return now to a consideration of the method used for finding the orientation of the principal crystallographic axes of the silver crystal. The crystal was clamped on a parallel plate and a fiducial or reference line scribed along its entire length using a sharpened tool. Having a reference line established, the crystal could be placed in the goniometer with its fiducial mark aligned to the zero index of the graduated circle on the goniometer head. With the gage set for a 3 centimeter separation of specimen and film, the position of the goniometer was adjusted so that the crystal just came into contact with the inner cylinder of the gage. At this point the gage was removed from the cassette and pin-hole system by releasing the

knurled screw in the outer cylinder.

A back reflection Laue photograph of the face centered cubic (f.c.c.) single crystal of silver is shown in Fig. 3. The circle at the center indicates the hole that is punched to allow the film to slip over the pin-hole system. An image of the pair of steel wires that was stretched across the film holder appear as cross-hairs on the photograph. It will be seen that the Laue spots lie on hyperbolic curves. The origin of the hyperbolic pattern is illustrated in Fig. 4. An unfiltered X-ray beam I from a molybdenum target passes through the photographic film at O, strikes the crystal at C, and gives a diffraction spot at P. The plane producing this diffraction spot lies in the zone[a] of which AE is the zone axis. If the line CP is allowed to rotate about point C keeping the angle θ constant, CP will describe a cone whose axis is AE. If the base of this cone is centrally projected from C on to the flat film M a hyperbolic curve is formed on the film. This is the basis of the geometric pattern of diffraction spots.

A cone of reflected rays is formed for each zone of planes in the crystal, and each cone intersects the film to form a row of spots lying on a hyperbola. The crystal-to-film distance CO and the angle OCP determine the position of the hyperbola QPN. Thus, the closest approach of the hyperbola to the center of the film is given by the

[a] All planes of a crystal which intersect along parallel lines are planes of a zone, and their intersection is the direction of the zone axis.

Fig. 3 - Back Reflection Laue Photograph of f.c.c. Silver Crystal. Principal Zones Are Indicated with Brackets. Principal Faces Are Shown in Parentheses.

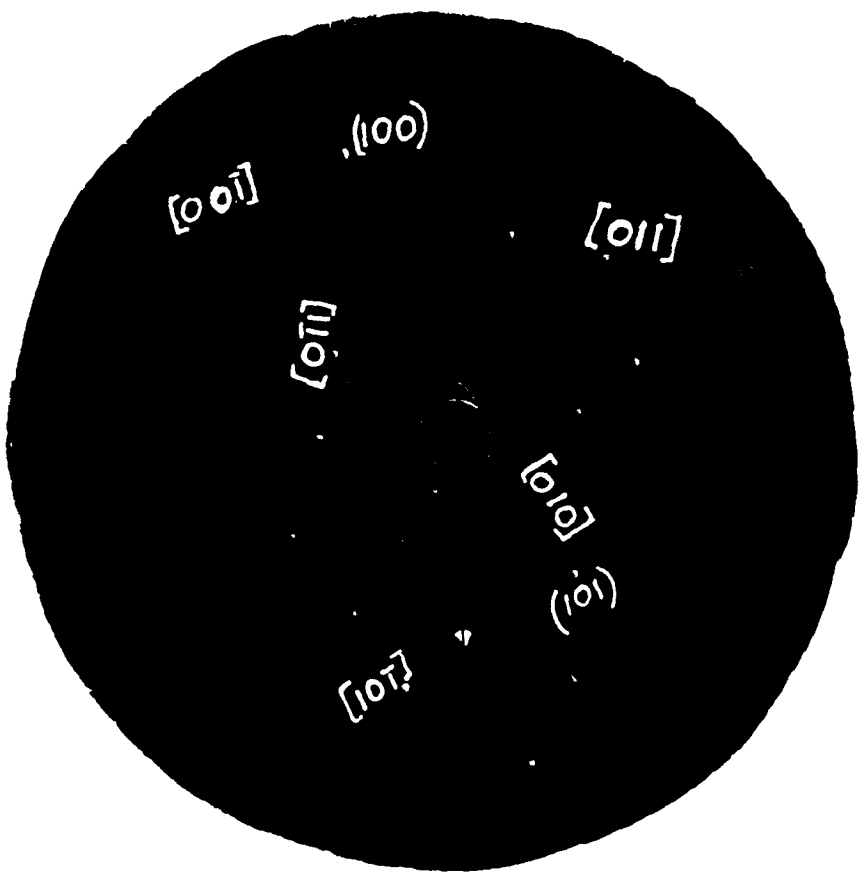
(100)
[001]
[011]
[01$\bar{1}$]
[010]
(101)
[10$\bar{1}$]

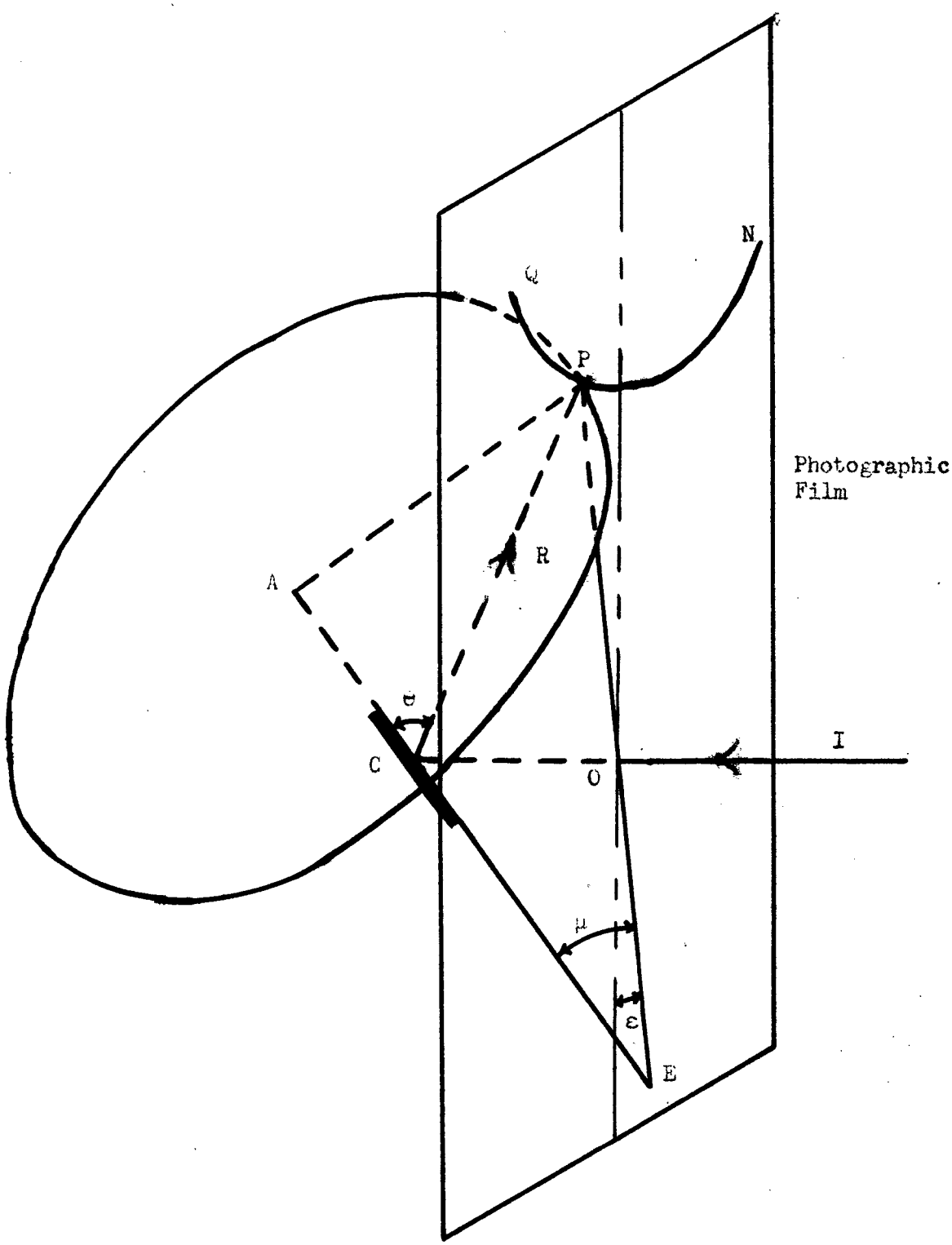

Fig. 4 - Hyperbolic Pattern of Back Reflection Laue Photograph.

relation

$$\overline{OP} = \overline{CO} \tan 2\mu \ .$$

If a zone axis such as AE is parallel to the film, the hyperbola will degenerate into a line passing through the center of the film. Further, each hyperbola is symmetrical with respect to the perpendicular projection of the zone axis upon the film.

Angular relations among the various zone axes in the crystal, corresponding to the hyperbolas appearing on the back-reflection photograph, can be read from a Greninger chart (24). Figure 5 shows a reproduction of a Greninger chart which was drawn for 3 centimeters separation of specimen and film; hyperbolas have been drawn for each 2 degrees of μ, Figs. 1 and 4. The angles μ and ε obtained from the chart for each zone are plotted on a Wulff net. True inter-zonal angles are measured by rotating the plot so that the two points representing zones lie on the same meridian of the net. With the two points on the same meridian, the angle between the points (reflections from crystal planes) is their difference in latitude, read directly from the latitude lines ruled on the net. A Wulff net ruled with two degree graduations is shown in Fig. 6.

Miller indices are assigned to each point in the plot by determining the angles between zones and comparing these angles with tabulated values. Tables of the angles between planes of two different indices (hkl) and ($h_1k_1l_1$) have been published (24) for crystals of the cubic system. A few of the more significant of these angles are listed

Fig. 5 - Greninger Chart Ruled for Intervals of 2 Degrees. Reduced in Size.

Fig. 6 - Wulff Net With 2 Degree Graduations.

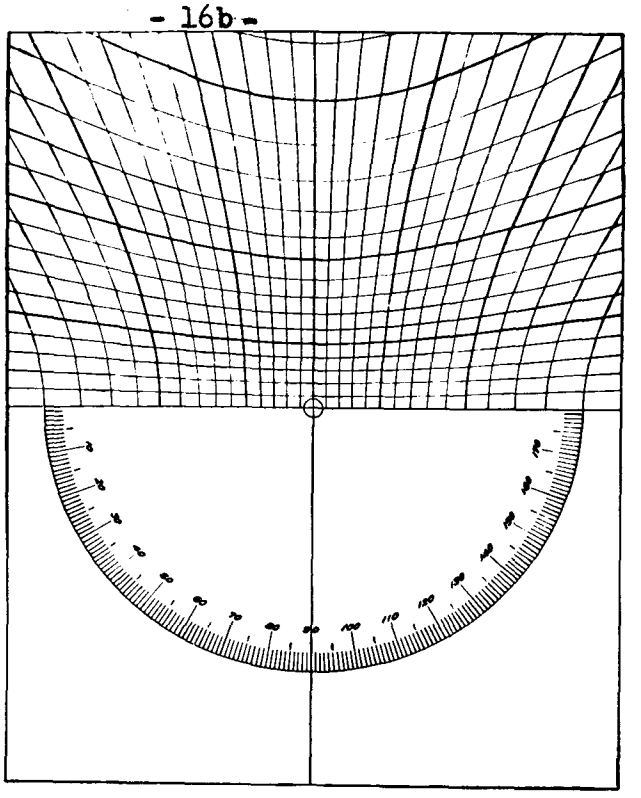

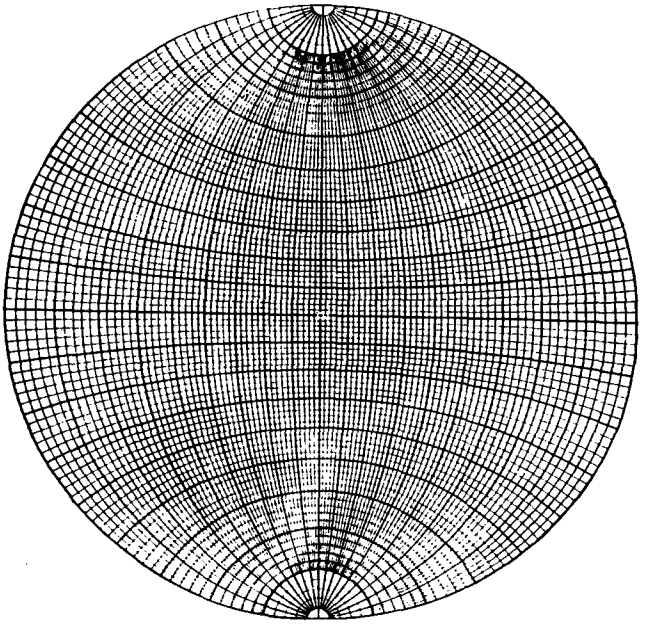

in Table 1. It should be mentioned here that in the cubic system the direction of the zone axis [hkl] is perpendicular to the plane (hkl) for all values of h, k, and l. Hence tables listing interplanar angles in this system give interzonal angles as well.

Using the method outlined above, the angles between crystallographic directions were measured on the X-ray photograph shown in Fig. 3. Indices were assigned to the various zones by comparing the measured values of Table 2 with the calculated angles in Table 1.

The spots at the intersections of the more prominent hyperbolas are reflections from the planes common to the principal zones. In Fig. 3 the (100) plane gives a strong reflection at the intersection of the [011] and [0$\bar{1}$1] zones.

As a check on the identification of the principal reflections, the silver crystal was rotated so that the X-ray beam was parallel to the [100] direction, or normal to the (100) crystal face. The symmetrical photograph shown in Fig. 7 was then obtained.

Since the [100] direction in a cubic crystal is a four-fold axis of symmetry, the diffraction photograph in Fig. 7 shows four-fold symmetry with respect to the X-ray beam. Thus with the crystal properly oriented, the back reflection Laue photograph exhibits the diffraction symmetry of the crystal axis that is parallel to the X-ray beam.

The photograph in Fig. 7 was taken with an exposure time of 50 minutes, using Ilford G, industrial X-ray film and a molybdenum tube operating at 50 kilovolts, 18 milliamperes. Standard 5-inch x 7-inch film was cut to a diameter of 5 inches and a hole punched in

Table 1. Calculated Angles Between Crystallographic Directions in Crystals of the Cubic System.

$[hkl]$	$[h_1k_1l_1]$	Angles between $[hkl]$ and $[h_1k_1l_1]$ directions		
100	100	0°	90°	
	110	45°	90°	
	111	54°44'		
110	110	0°	60°	90°
	111	35°16'	90°	

Table 2. Angles Measured Between Zones of f.c.c. Silver Crystal From X-ray Photograph Shown in Fig. 3

$[hkl]$	$\varepsilon_{(hkl)}$	$\mu_{(hkl)}$	$[h_1k_1l_1]$	Angle between $[hkl]$ and $[h_1k_1l_1]$
011	20°	21.5°	010	45°
			$0\bar{1}1$	90°
			$00\bar{1}$	45°
			$10\bar{1}$	60°
010	62.5°	4.2°	$0\bar{1}1$	45°
			$00\bar{1}$	90°
			$10\bar{1}$	90°
$0\bar{1}1$	-76.5°	15.2°	$00\bar{1}$	45°
			$10\bar{1}$	60°
$00\bar{1}$	30.5°	26.5°	$10\bar{1}$	45°

Fig. 7 - Laue Photograph of Silver Crystal Before Cutting. X-ray Beam Parallel to Four-Fold Axis of Symmetry.

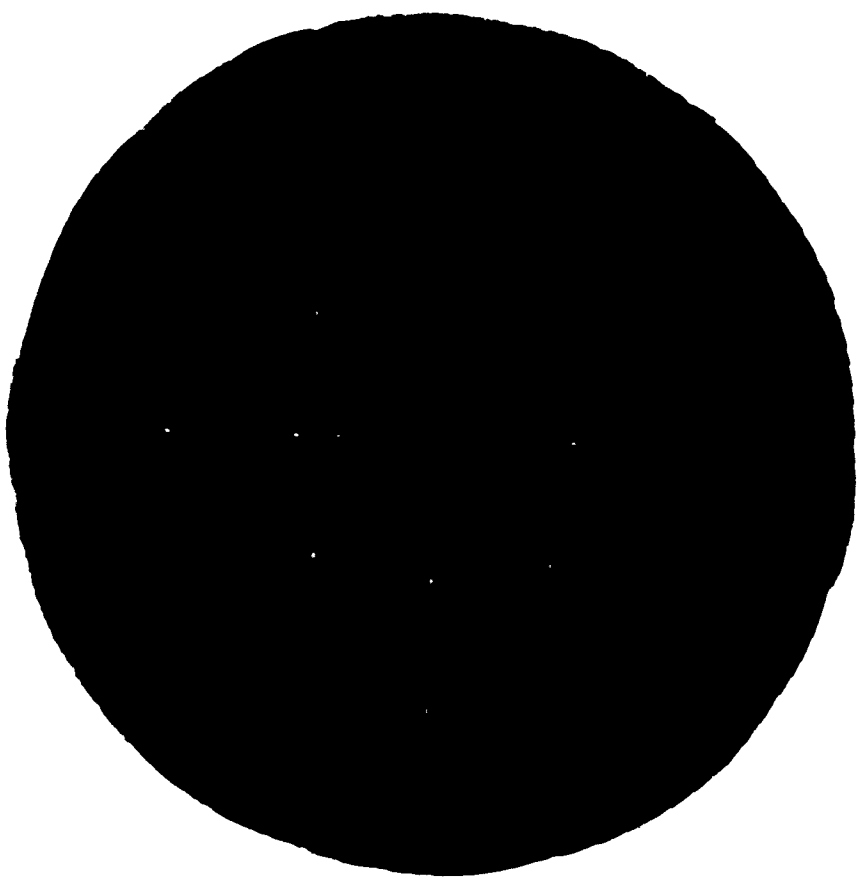

the film to fit over the pin-hole system. Both the direct and reflected beams were unfiltered. The crystal-to-film distance was 3 centimeters.

It has been established in Fig. 7 that the X-ray beam is parallel to a principal four-fold axis of symmetry of the silver crystal. The vertical row of spots in the same photograph was indexed as the [110] zone. This suggests that a horizontal axis perpendicular to the X-ray beam is a two-fold axis of symmetry of the crystal. Figure 8 was taken after rotating the goniometer 90 degrees about its vertical axis from the position which gave the pattern in Fig. 7. The photograph shown in Fig. 8 thus verifies the identification of the zone indices in Fig. 7. The goniometer angles corresponding to the positions of the specimen in Figs. 7 and 8 completely specify the orientation of the silver crystal.

A fourth photograph was taken with the goniometer rotated through an angle of 54°44' about its vertical axis from the position in Fig. 7. In this position of the crystal, the X-ray beam is directed along a body diagonal of the cubic unit cell. Figure 9 shows the three-fold symmetry of this axis.

The geometry of these various rotations can be illustrated from Fig. 10. AEG represents the fundamental building block or unit cell of the face centered cubic crystal of silver. Typical two- three- and four-fold axes of symmetry are shown parallel to BD, AF, and BC, respectively. The angles between these axes are given in Table 1.

Fig. 8 - Laue Photograph of Silver Crystal Before Cutting. X-ray Beam Parallel to Two-fold Axis of Symmetry.

Fig. 9 - Laue Photograph of Silver Crystal Before Cutting. X-ray Beam Parallel to Three-fold Axis of Symmetry.

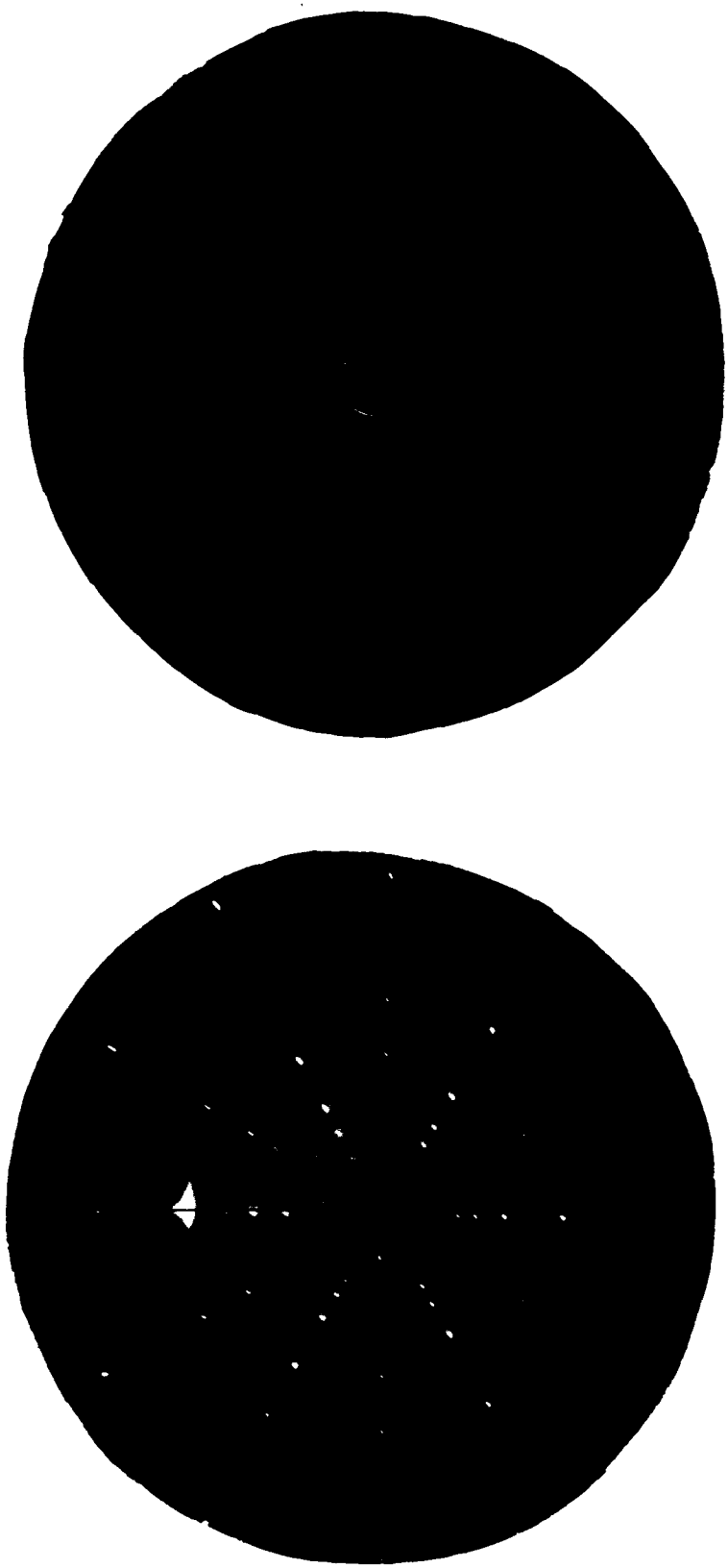

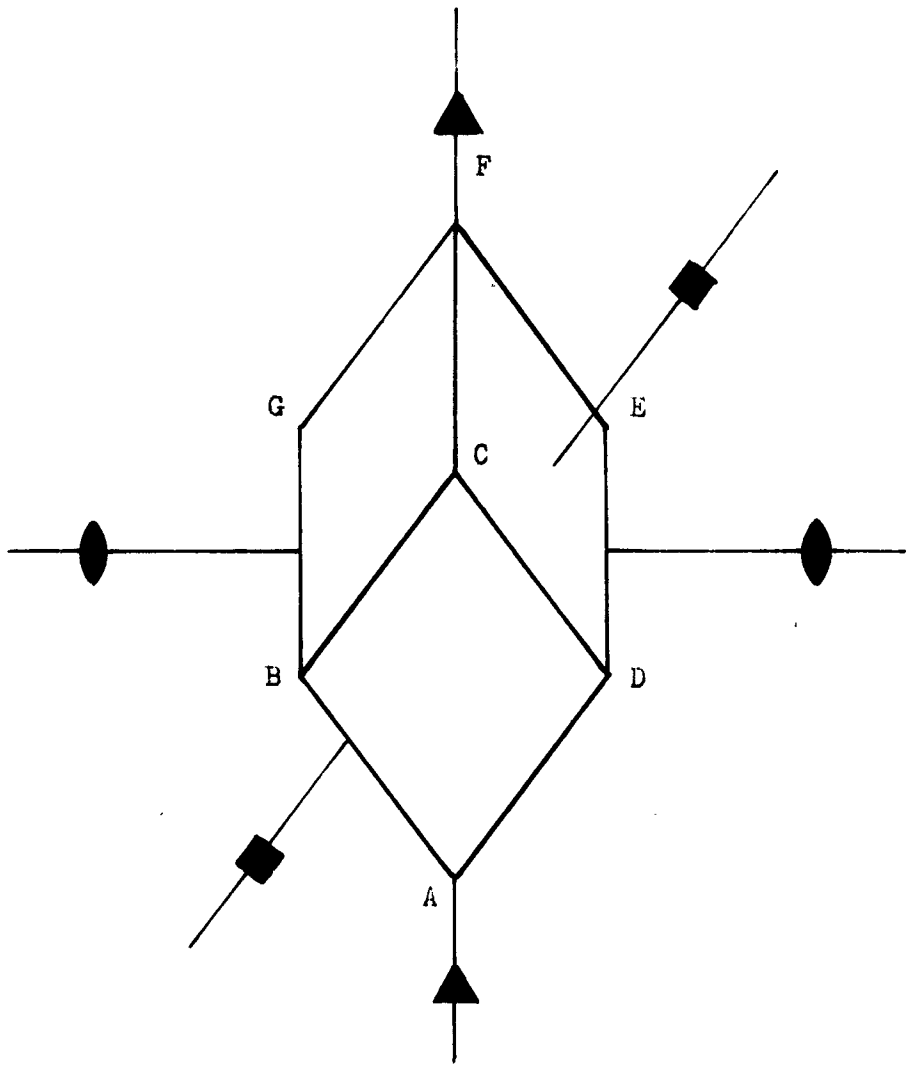

Fig. 10 - Unit Cell of Cubic Crystal Showing Two-, Three- and Four-fold Axes of Symmetry.

B. Cutting and Polishing Single Crystals of Silver and Rocksalt

One of the important considerations in studying surfaces is to obtain surfaces of known configuration. An electrolytically polished surface along a known crystal plane is one of the nearest approaches to a known surface. The aim here is to obtain a surface that is atomically smooth. Of course, no surface is completely smooth, and impurities cannot be entirely removed; but it is an approach to a surface of known configuration.

1. Machining of Silver Crystal

A surface parallel to a (100) plane of the f.c.c. crystal of silver was prepared in the manner described below. The specimen was clamped in a 5/8 inch draw-in collet of a Type BB4, Hardinge Brothers precision milling machine, and the angles designated as α, β, and γ in Appendix A set at zero degrees on the Index Center. Also the fiducial mark that had been previously scribed along the length of the crystal, as well as the index of the traverse on the milling machine were aligned with the axis of the saw or cutting tool. The axis of the saw then bears the same relation to the crystal rod as did the X-ray beam, with the crystal mounted in the goniometer.

The saw used was 3 inches in diameter and .022 inch thick, and had a tooth pitch of 1/8 inch. With the set screws of each of the

axes of the milling machine released, the crystal rod could be revolved about its own longitudinal axis (α), about an intermediate horizontal axis (β), and about the vertical axis of the Index Center ($\uparrow$). After the Euler angles α, β, and $\uparrow$ were set to expose the desired plane, the set screws were clamped tightly against the holder and the plane of the saw was then parallel to one of the (100) planes of the crystal.

By moving the table which carried the Index Center of the milling machine, the crystal was brought into contact with the saw. A cut was made through the crystal rod with the saw revolving at a speed of 400 revolutions per minute. A second plane, different from the first, could be cut on the same rod by setting the Euler angles to the new values as calculated in Appendix A. During the cutting operation, the crystal was lubricated with friction-proofing oil. Immediately after cutting, the crystal face was cool when placed to one's lip, showing that very little heat had been produced by the cutting.

2. Polishing of Silver Crystal

Machining of the single crystal of silver leaves a disrupted layer of metal at the surface. The back-reflection Laue photograph along the [110] direction in Fig. 11 was taken after sawing the crystal rod but before any further treatment of the specimen. Continuous rings indicate the random orientation of the crystallites at the surface as a result of the machining process.

Fig. 11 - Laue Photograph of Silver Crystal Face After Cutting But Before Electropolishing. X-ray Beam Normal to Machined Face.

Fig. 12 - Laue Photograph of Silver Crystal Face After Electropolishing. X-ray Beam Parallel to Two-fold Axis, Normal to Polished Surface.

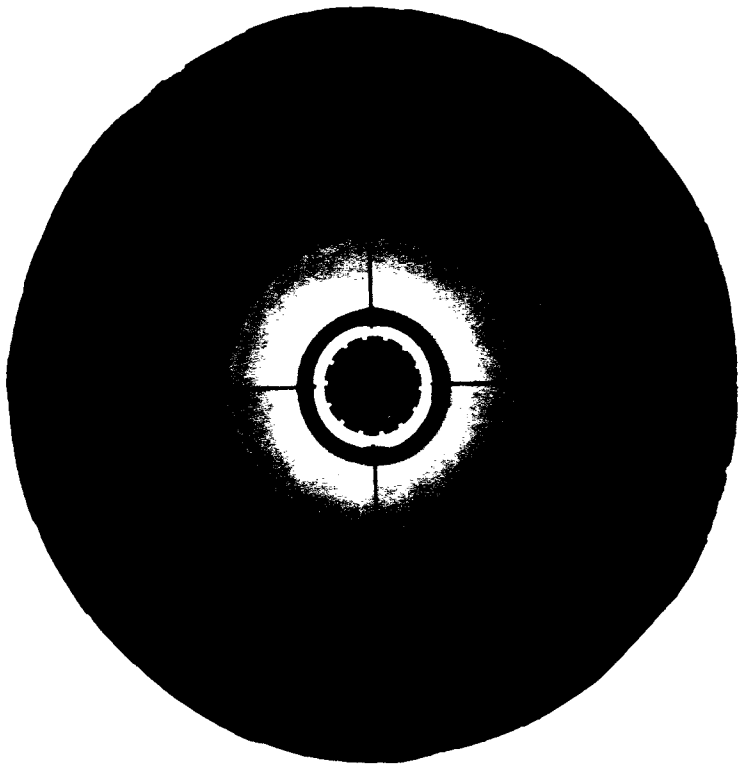

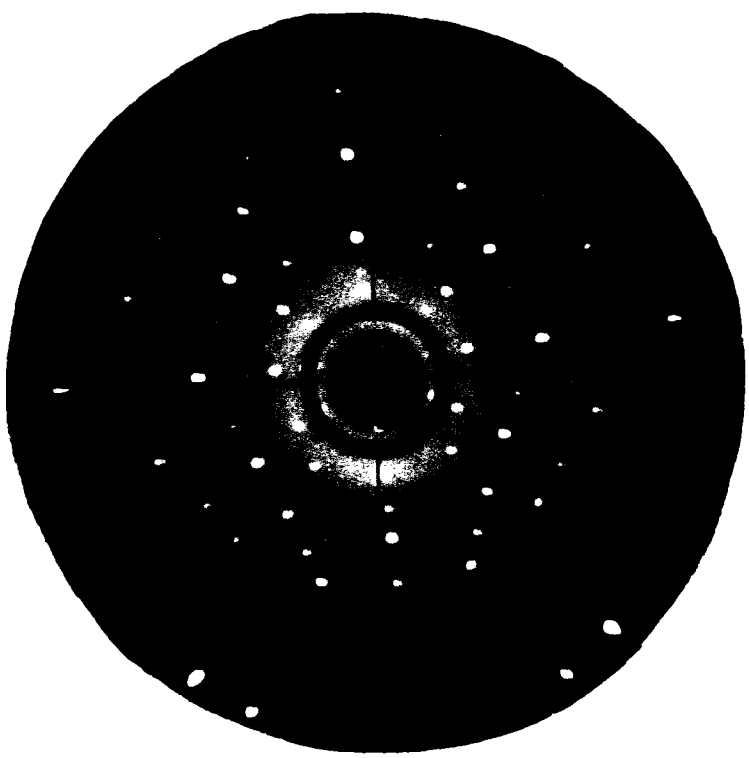

The milled surface of the crystal was made plane by mechanically polishing on Nos. 1, 0, 2/0, 3/0, and 4/0 metallographic polishing papers placed on a piece of plate glass. Between the successive mechanical polishes, the surface was swabbed with a soft tissue under a stream of water. This treatment removes any grit left on the surface by one paper before sanding on the next finer grade.

Mechanical polishing with even the finest emery paper leaves the surface lightly scratched and produces a disturbed layer on the surface of the crystal. A very bright and smooth finish was obtained by electrolytically polishing the specimen in a cyanide solution using the method employed by Gilbertson and Fortner (25). The electrolytic method has the advantage of removing any disrupted metal simultaneous with the polishing.

The electrolytic cell used in the polishing is shown schematically in Fig. 13. The cell consisted of a 600 milliliter beaker and a cylindrical copper cathode .025 inch thick. The mechanically polished silver crystal served as anode and was supported downward with a No. 14 AWG solid copper wire. Best polishing results were obtained at a current density of 20 milliamperes per square centimeter for one hour and a voltage drop of 1.2 volts across the cell. At slightly higher current densities a white or slightly gray film formed on the surface. When the current density was increased to 40 milliamperes per square centimeter, the crystal face became roughened. At low current density the (100) face gave a matte appearance characteristic of electrolytic etching.

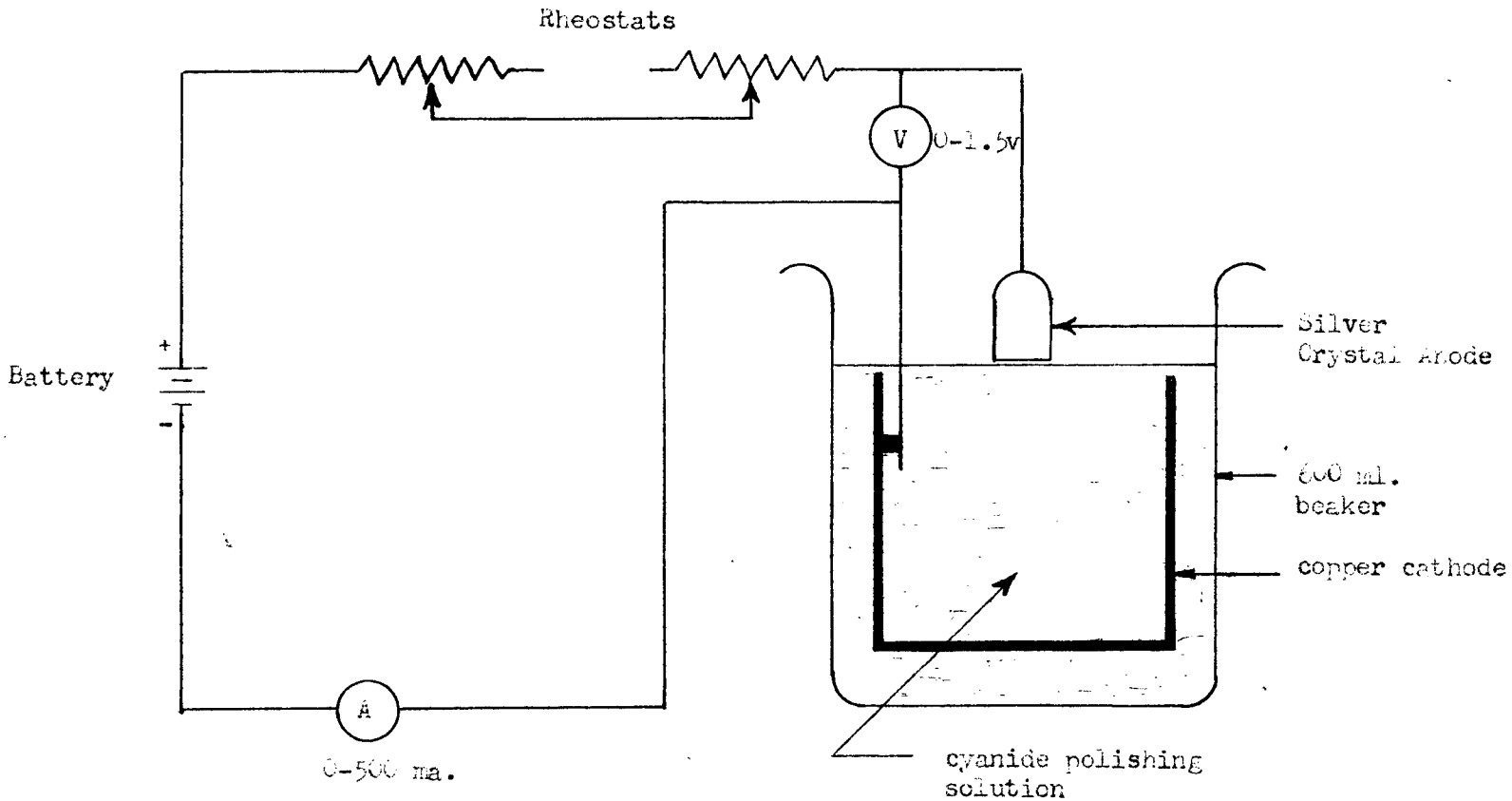

Fig. 13 - Apparatus and Circuit Diagram for Electro-polishing Silver Crystal.

A freshly prepared polishing solution produced the smoothest surface. After the circuit was closed by lowering the crystal into the electrolytic cell, the current density was gradually increased by adjustment of the series rheostats until the first current and voltage fluctuations were noted. The current density was then maintained at this point until the desired degree of polish was obtained. During the interval at which polishing occurred, an orange-brown film alternately formed and dissolved at the crystal (anode) surface. Fluctuations of the current and voltage followed the formation and dissolution of the anode film. In the absence of this film no polishing action was observed. Jacquet (26), and Epelboin and Chalin (27) have discussed the mechanism of electro-polishing of metals as well as the optimum cell conditions of voltage and current density during the polishing. They report that the anode film always formed when polishing took place.

Sometimes it was found that after the electrolytic polishing had been completed, light scratches left from the initial sanding on metallographic paper could be seen with a microscope. In such cases, the surface was again rubbed on the 4/0 paper followed by a second electro-polish. This process was repeated until a brilliant and smooth surface was obtained. At the end of the polishing period, the silver crystal was removed from the electrolytic polishing bath and given a quick rinse in distilled water followed by dehydrating in absolute ethanol.

Proof of the single crystal character of the surface was obtained

by mounting the specimen inside the electron diffraction camera and observing the characteristic single crystal pattern on the fluorescent screen. This procedure and the results will be described in a later paragraph. A back reflection Laue photograph of the electro-polished surface is shown in Fig. 12.

3. Polishing of Rocksalt Crystal

Metallic films can be deposited on rocksalt and the salt crystal subsequently dissolved in distilled water leaving the film accessible for further study.

Natural crystals of rocksalt were polished by a procedure similar to the procedure used in polishing metal surfaces or crystals. A clean surface was obtained by cleaving the crystal from a larger specimen. Crystals of rocksalt that are more than 1/4 inch thick are more easily cleaved by using a sharp knife and hammer; crystals less than 1/4 inch thick can be nicely cleaved with a razor blade.

The sharpened edge of the blade is placed in position on the block crystal and the back of the blade is then given a sharp tap with the hammer. This cleaves the crystal along a cube face. The freshly cleaved face will usually be 'stepped' or irregular and can be smoothed by rubbing successively on No. 1 to No. 4/0 metallographic emery paper.

After polishing the crystal with the emery papers, the surface takes on a ground-glass appearance. The surface was given a final polish by rubbing lightly on a clean blotter that had been wetted with

distilled water. This latter treatment produced a clear, smooth surface. The crystal was then rinsed in absolute ethanol to remove the excess moisture and placed in a dust-free atmosphere (bell jar) to dry.

Natural crystals of rocksalt were obtained at a very nominal cost from Ward's Natural Science Establishment, Rochester, New York. Specimens that were more optically clear were selected and crystals approximately 1 centimeter on edge were cleaved from the blocks by the method described above.

C. Evaporation of Molybdenum on Single Crystals of Silver and Rocksalt

Thin metal films prepared by vacuum evaporation are used in the production of optical mirrors and in the preparation of getter layers. Metals of the sixth group and the alkaline earth metals, used in the production of electronic tubes, evaporate at high temperatures in vacuum and condense on the walls of the envelope. Electron diffraction studies of thin layers produced by evaporation have yielded quantitative, as well as qualitative, data about the structure of these films. The diffraction studies made with thin films in the present experiments together with the experimental methods will be described in the paragraphs that follow.

1. The Vacuum System

In the preceding section it was pointed out that atomically clean surfaces are of the greatest importance in studies of surface layers. Not only must the surface be prepared with a known configuration but care must be taken to keep the surface free of contamination during subsequent experiments, particularly during the deposition of films by evaporation in vacuum. This requires the maintenance of the best vacuum that can be obtained.

Figure 14 shows a schematic cross section of the evaporation tube and the apparatus used for producing the vacuum. At the left of the diagram is shown the fore pump and a mercury diffusion pump. The fore pump was a Welch DuoSeal vacuum pump capable of reducing the pressure to approximately 10^{-3} millimeter of mercury. Lower pressures were obtained with the mercury diffusion pump. The action of the diffusion pump is similar to a spray gun. Mercury vapor generated in the boiler is directed downward through a nozzle. The vapor molecules then collide with gas molecules from the system to be evacuated. The gas molecules are driven into the fore vacuum chamber and are expelled into the atmosphere by the fore pump.

Most of the mercury vapor condenses on the side walls of the pump and is returned to the boiler. However, some of the molecules diffuse backward toward the system being evacuated. These are prevented from reaching the system by being condensed in the cold trap (center) consisting of a mixture of dry ice and acetone (-78°C).

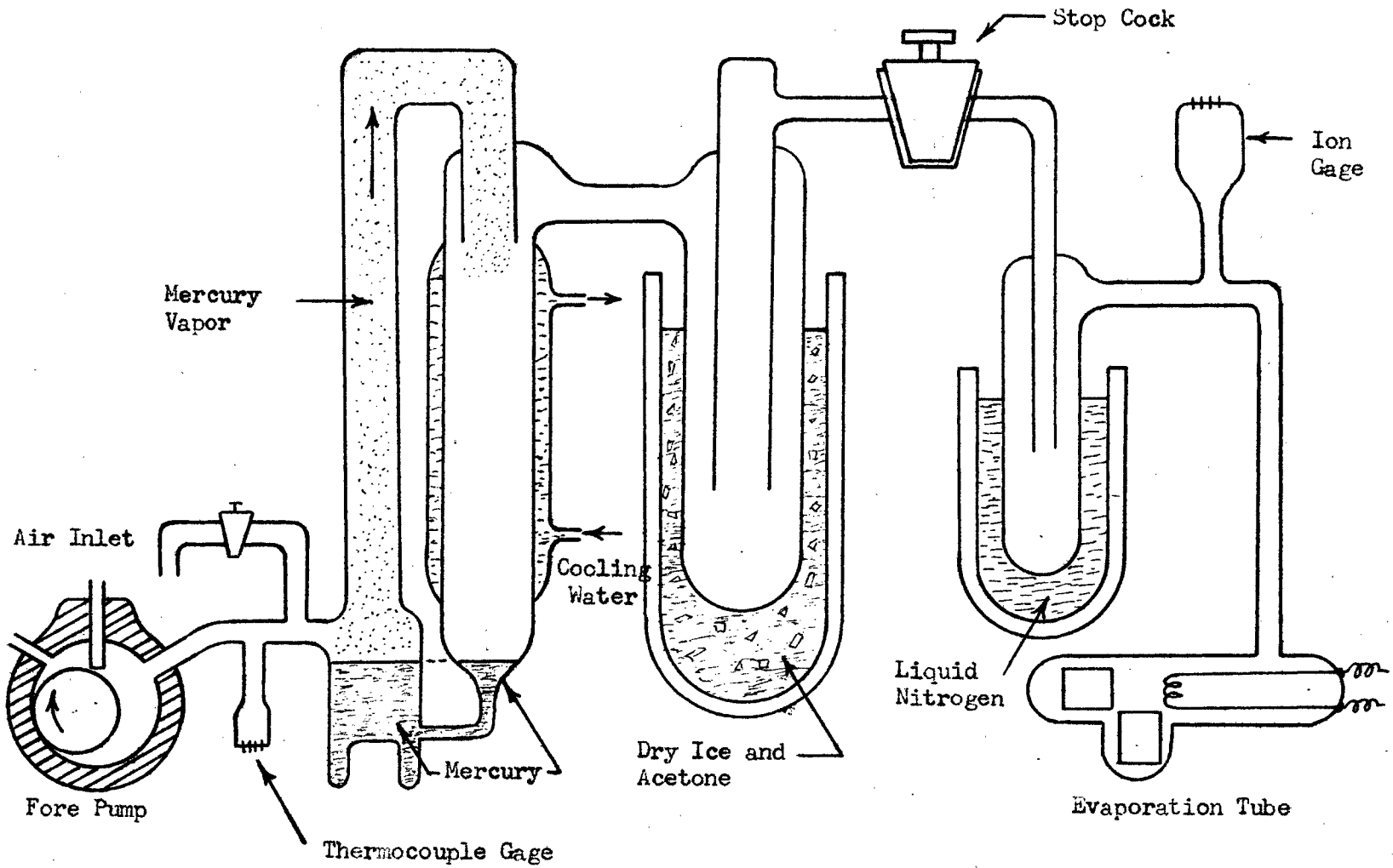

Fig. 14 - Schematic Drawing of Mercury Diffusion Pump and Associated Vacuum Apparatus.

Gases such as carbon dioxide and water vapor are condensed in the liquid nitrogen trap (-195°C) at the right of the diagram. Vapors given off by the vacuum grease used on stop cocks and at the rubber-to-glass junctions were also effectively trapped by the liquid nitrogen.

Two gages were used for measuring the pressure in the system. A thermocouple gage measured the fore-vacuum pressure. The pressure at the evaporation tube was measured with a type 05-700 ionization gage manufactured by the National Research Corporation.

Leaks in the glass vacuum system were located by passing the high voltage terminal of a Tesla coil along the glass surface. If a leak existed, a well-defined discharge formed at the terminal, and the air inside the glass tube became ionized. If no leak was present, only a few scattered stramers could be observed at the high voltage terminal as it was moved over the glass surface.

2. The Evaporation Tube

At the lower right of the diagram in Fig. 14 is shown the vacuum evaporation tube. A sketch of this tube in which thin films of molybdenum were prepared is shown diagramatically in Fig. 15. The evaporation tube was a flat-bottomed cylindrical pyrex tube having an inside diameter of 3/4 inch. It was connected to the vacuum system by means of the T-piece near the top. Two tungsten wires, each 0.050 inch in diameter, were sealed through the pyrex at the top using

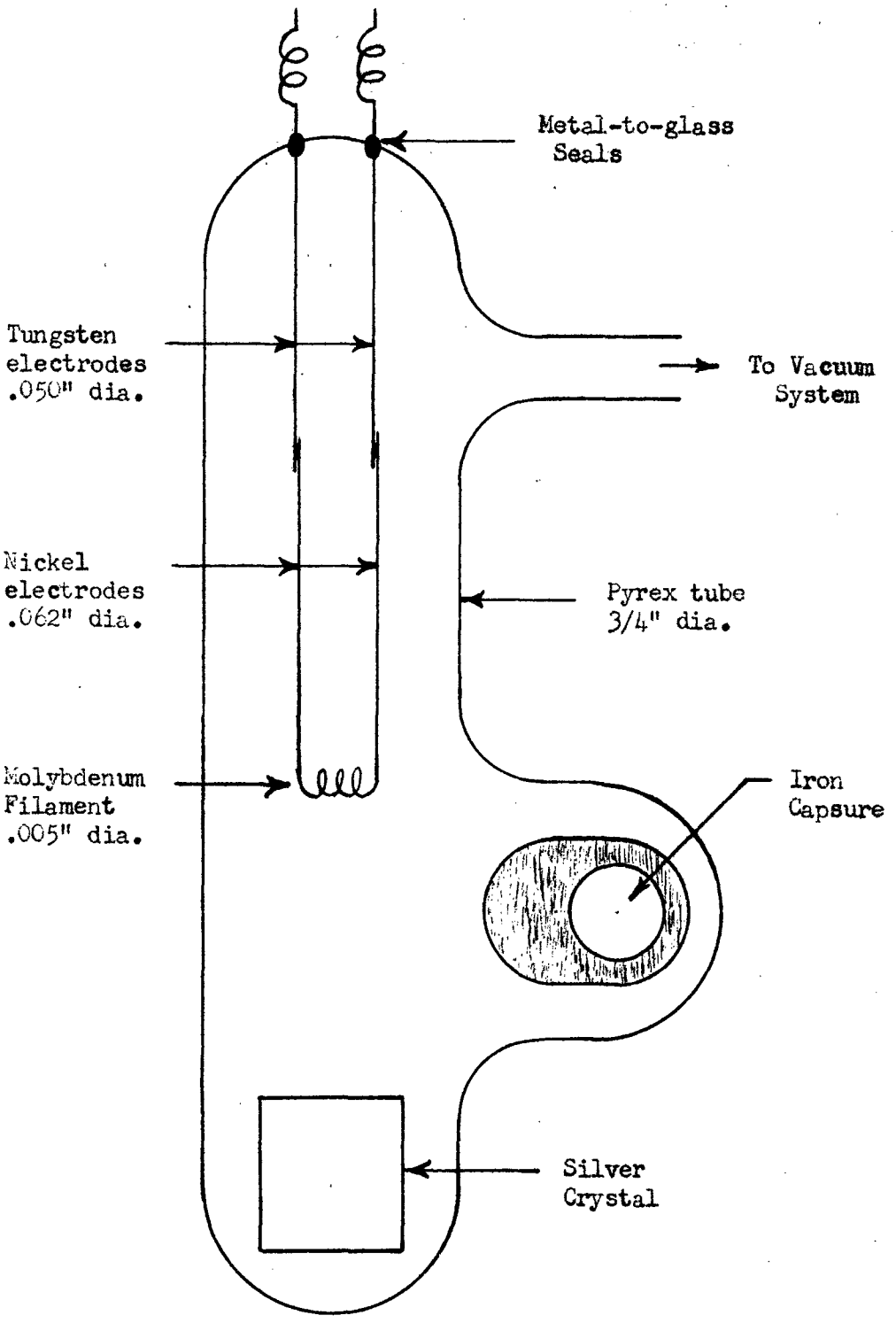

Fig. 15 - Diagram of Pyrex Tube Used for Evaporation of Molybdenum.

nonex glass seals. Nickel wires 0.062 inch in diameter were spot welded to the tungsten electrodes inside the tube, and the molybdenum filament was spot welded to the ends of the nickel wires.

The filament was in the form of a helix and consisted of six turns of 0.005 inch molybdenum wire wound with a pitch of one turn per millimeter. The total length of the filament wire was 6.5 centimeters. A 1/8 inch mandrel was used as a core around which the coil was formed. Complete information on the design of the molybdenum filaments will be found in Appendix B.

In agreement with the findings of other workers (28) it was found that the molybdenum filaments could not be welded directly to the tungsten electrodes. It has been suggested that this was due to the rapid formation of oxides when these metals are heated in air. Further, good bonding at welded joints can only be obtained when the metals to be welded are very clean and the pure metals are in intimate contact at the joint. Nickel was therefore used as a flux to dissolve the oxides formed during welding. Nickel rods, with which molybdenum forms a good bond, were welded to the lead-in tungsten electrodes and the molybdenum filament was in turn spot welded to the nickel rods. A good bond was obtained when the current density at the welded joint was neither very high nor very low. With a Variac set to give the proper welding current, the parts to be welded were held under pressure by the welding (copper) electrodes and the primary circuit energized. When the metals reached the plastic state, the

primary circuit was opened. Pressure was maintained on the joint until the electrodes had cooled and the weld became permanent.

A soft iron pellet was sealed inside a pyrex capsule located between the filament and the crystal surface within the evaporation tube. During the initial evaporation, possible contaminating elements from the heated filament were prevented from reaching the crystal by the pyrex capsule. After the evaporation had proceeded for some time (4 or 5 minutes) at reduced current, the iron pellet was magnetically attracted toward the side chamber, thus removing the capsule from between the filament and crystal. The single crystal (silver or rock-salt) rested on the bottom of the tube with its (100) surface facing toward the filament.

Heat from the filament as well as from the electric furnace prevented the use of rubber gaskets in the construction of the tube. This made it necessary to cut the pyrex tube in order to replace the filament and remove the crystal after depositing a molybdenum film.

3. Preparation of Thin Films of Molybdenum

(a) Molybdenum Film Deposited on Rocksalt. Thin films of molybdenum were prepared on the (100) face of a natural sodium chloride crystal by heating a molybdenum filament in the vacuum system in Fig. 14 for approximately three minutes at 2.25 amperes. The distance between the molybdenum coil and the cleavage plane of the sodium chloride crystal was about 2.5 centimeters. The pyrex tube was

evacuated by the system described, and then heated in an electric furnace. When the furnace temperature reached 300 degrees centigrade, the molybdenum was evaporated by maintaining a current of 2.25 amperes through the coil until the filament burned out. A mercury-in-glass thermometer was used to measure the temperature of the furnace. The pyrex tubing leading from the liquid nitrogen coldtrap to the furnace was outgassed by heating in a soft flame for twenty minutes.

After a molybdenum film had been evaporated onto the rocksalt crystal, the furnace was removed from the tube and the tube allowed to cool in air. Upon removing the salt crystal from the evaporation tube, the crystal was again cleaved to give two specimens of the molybdenum film for further experimental work. Each film surface thus obtained was approximately 5 millimeters square.

The molybdenum film was removed from the surface of the rocksalt by the following procedure: One drop of 5 percent collodion (one cc collodion in twenty cc N-amyl acetate) was placed on the metal film and allowed to completely dry in a dust free atmosphere. The crystal was then placed in a shallow glass dish with the metallic film on the top face of the crystal. Distilled water was added to the dish until the water level became flush with the top of the crystal. In a few minutes the film (attached to the collodion) floated free of the salt crystal which had partially dissolved. The film was then picked up from underneath on a 200-mesh stainless steel wire gauze. Excess water between the film and the gauze was removed by touching a soft tissue to the gauze. The film had a good metallic lustre.

It was found that films that are thin enough to give electron diffraction patterns by transmission are extremely fragile and must be handled with the greatest care to prevent their disintegrating.

(b) Molybdenum Film Deposited on Silver. The apparatus in which a thin film of molybdenum was prepared on a silver crystal was the same as that for depositing molybdenum on rocksalt. Molybdenum was evaporated from a molybdenum wire 6.5 centimeters in length and 0.005 inch in diameter wound in a coil having six turns. The coil was heated in vacuum at a current of 2.2 amperes for three minutes when the coil burned out. The distance between the filament and the (100) face of the silver crystal was about 4 centimeters.

After evacuating the pyrex evaporation tube, the tube was inserted into the electric furnace and heated to a temperature of 350 degrees centigrade. A molybdenum film was evaporated on to the silver crystal by the current through the molybdenum coil. The furnace was then removed and the tube allowed to cool to room temperature. During evaporation the pressure was approximately 10^{-4} millimeter of mercury.

The structure of the molybdenum films was investigated with the electron diffraction instrument. Films deposited on the sodium chloride crystal were examined by the transmission method of electron diffraction, while the film evaporated onto silver was studied by the reflection method.

4. Determination of Film Thickness

The orientation of the crystals in thin layers has been observed to be related to the thickness of the layer (19). Measurements of film thicknesses would therefore be an important part of the study of films condensed from the vapor. Of the methods that have been used to determine the thickness of evaporated films, the multiple-beam interferometer is perhaps the most direct. This was the method employed in the present experiments for measuring the thickness of the molybdenum film deposited on rocksalt.

The film used in making thickness measurements was obtained by attaching a thin glass microscope slide, 1 centimeter by 0.5 centimeter, on the surface of the salt crystal nearest the filament within the evaporation tube. As the glass slide covered only one-half of the surface of the crystal, the thickness of the film deposited on the slide should be the same as on the crystal. Molybdenum was thus condensed simultaneously on the microscope slide and on the crystal by evaporation from a 0.005 inch filament in the vacuum system described above.

The optical arrangement used for the interferometric measurements of film thickness was similar to the arrangement employed by Bearinger (29) in measuring the thickness of gold films. Interference was obtained between a silver film deposited on glass and another silver film deposited over the molybdenum film whose thickness was to

be measured. An f/6.3 camera lens operated at full aperture was focussed on infinity, and a point source of light from a high pressure mercury vapor arc placed at the focal point of the lens. A Wratten No. 61 filter placed in front of the camera lens selectively transmitted the 5461 Angstrom unit line of mercury. The interference pattern was adjusted by varying the pressure on the metal plates holding the microscope slides. An ordinary light microscope was used to observe the fringes. The pattern was photographed on 3 1/4 inch by 4 1/4 inch, Tri-X Kodak film with an exposure time of three minutes. Figure 16 shows the interferogram that was obtained.

The separation of the fringes d, and the fringe shift x, included within the area marked by the white lines on the photograph, were measured using a Bausch and Lomb optical eyepiece with built-in millimeter scale. The film thickness was then calculated from the equation

$$t = \frac{\text{fringe shift, } x}{\text{fringe separation, } d} \times \frac{\text{wave length of incident light}}{2}$$

All of the silver films were deposited in a type EMV-1A RCA Vacuum unit by evaporating silver from pieces of silver wire, each one-half inch long, suspended from the loops of a heated tungsten filament. This filament was formed by winding 0.040 inch tungsten wire into a helix of six turns on a spindle 3/8 inch in diameter. As tungsten wire is extremely brittle at room temperatures, it was

Fig. 16 - Interference Fringes Showing the Shift Produced By a Metal Film Approximately 500 A.U. in Thickness. Wavelength of the Incident Light Was 5461 A.U.

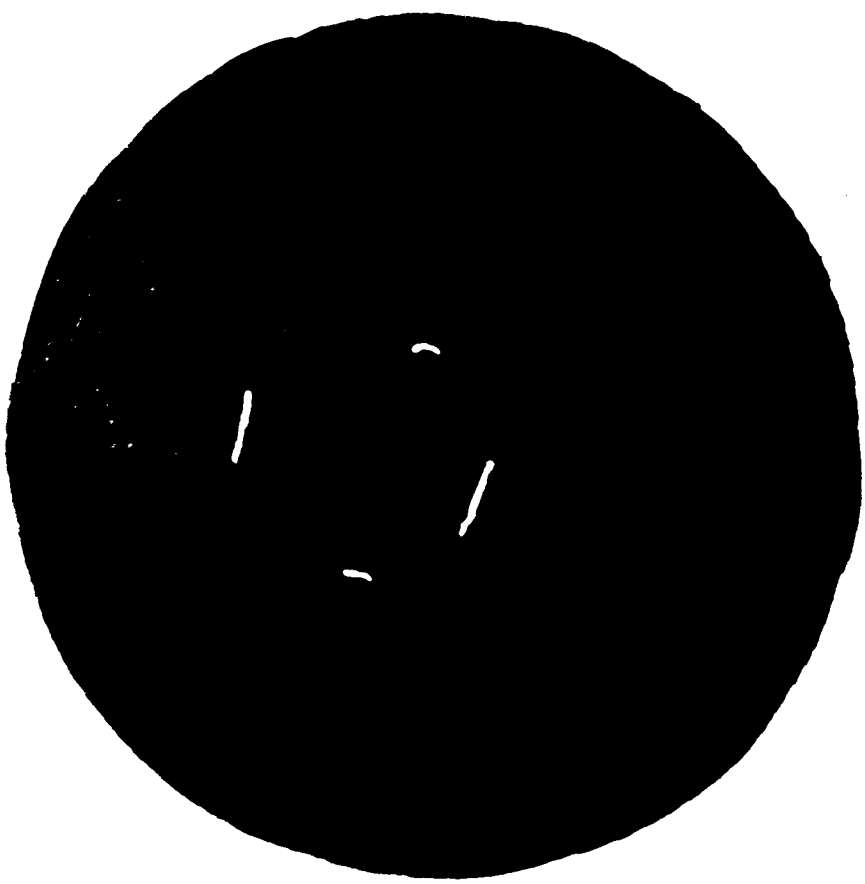

necessary to heat the wire slightly in warm water (50° - 60° C) immediately before forming the filament. The evaporation chamber was pumped to a pressure of less than 10^{-4} millimeter of mercury and the current in the tungsten filament was slowly increased to 14 amperes. At this current, it could be seen that the silver wires had melted and formed small beads on the tungsten filament. Evaporation was continued for approximately half an hour, until none of the silver remained on the filament.

The molybdenum film slide was placed at a distance of 1-1/2 inches from the filament in the chamber, in order that the silver film deposited on this slide would render the slide opaque. Before evaporating the silver a step was formed in the molybdenum film by drawing a dull needle across the microscope slide on which this film had been deposited. The glass microscope slide, on which a silver film was to be deposited to give 8 percent light transmission, was thoroughly washed in a detergent, rinsed in hot distilled water, washed and rinsed again and allowed to dry in a dust free atmosphere before being placed in the evaporation chamber.

D. Structure of Evaporated Films

1. Electron Diffraction Instrument

All of the electron diffraction patterns were taken with a beam energy of 40 kilovolts, using a General Electric, Type G2 Electron Diffraction Instrument.

The instrument consisted of the electron gun tube for accelerating and collimating the electron beam, adjustable magnetic focusing coil wound concentric with the tube, specimen chamber and specimen manipulator, shutter, and photographic plate housing. A high-voltage power supply which furnished the accelerating voltage to the electron gun was variable from 20 kilovolts to the maximum. The source of electrons was a hot tungsten cathode. Two apertures, one 0.003 inch in diameter near the cathode and the other 0.002 inch in diameter in the anode, acted as the collimating system. With the specimen withdrawn from the electron beam, the beam was focussed into an intense spot on the fluorescent shutter by means of the magnetic focus coil.

After being diffracted by a crystal specimen, the scattered electron beam diverged into the cone of the camera chamber and impinged on either a fluorescent viewing screen or on the photographic plate.

The vacuum system, including the electron gun, specimen chamber, and camera housing, was continuously evacuated through the specimen box. A Welch Duo-Seal vacuum pump was used as the mechanical fore pump. The diffusion pump was a vertical, water-cooled, oil pump using

silicone fluid. Vacuum in the line connecting the specimen box and the oil diffusion pump was indicated by a thermocouple gage. A remotely controlled solenoid vacuum valve was used to isolate the vacuum system from the pumps during specimen changes or during the loading and unloading of the camera. The instrument was completely self-contained and was mounted in a movable, desk-type structure.

Before significant and reproducible diffraction patterns could be obtained, it became necessary to make a number of modifications in the design of the instrument. All of the flat rubber gaskets used as vacuum seals on moving parts (push buttons, shutter, specimen manipulator, etc.) were replaced with Linear O-Ring seals. The glass-constructed, air-cooled, oil diffusion pump was replaced with a water-cooled metal pump. This eliminated the problem of breaking the Kovar-to-glass seal when it was necessary to remove the diffusion pump for maintenance purposes.

In the usual design, the specimen manipulator was mounted in the top plate of the specimen box. This seemed to be an excellent location for a liquid-air cold trap. A cold trap was therefore constructed and installed in the top plate of the specimen chamber. In the later operation of the diffraction instrument, it was found that the cold trap improved the vacuum by a factor of eight to one. The specimen manipulator was placed in the bottom plate of the chamber, and the functions that were previously performed from the bottom plate were located elsewhere on the box. A type 05-700, National Research Corporation ionization gage was also mounted on the specimen box. This

gave a continuous indication of the pressure near the specimen being examined with the electron beam.

By means of a helium leak-detector manufactured by the Consolidated Engineering Company, it was found that a crack had developed in the soldered joint connecting the cone with the camera housing. A satisfactory vacuum (10^{-5} mm of Hg) was obtained after this joint was sealed with Apiezon Q vacuum compound.

A fluorescent mixture for coating the shutter screen was prepared and applied to the screen in the following manner. The procedure followed somewhat the method outlined in the RCA Electron Microscope Manual (30). Two grams of Type 33Z605B powdered phosphor obtained from RCA was ground in an agate mortar and pestle to reduce the particle size. A binder solution was prepared of one cc nitrocellulose and three cc N-amyl acetate. The powdered phosphor and the binder solution were placed in a 25 milliliter beaker and the mixture stirred with a glass rod until a uniform suspension was obtained. This suspension was poured on to the metal plate and spread around by tilting the plate until the plate was completely covered. The shutter was then placed in a dust free area and allowed to dry. A good quality of fluorescent screen was obtained by this method.

2. Electron Diffraction Patterns

Identification of the reflections that appear on an electron diffraction pattern is made by calculating the d-spacing in the Bragg

law for each reflection and comparing the calculated d-values with published results of d-spacings for known compounds (31). The d-spacing is directly related to the diameter of the diffraction rings in the pattern of a polycrystalline specimen. It is related in a similar manner to the separation of the observed reflection and the central spot of a single crystal diffraction pattern. These relationships can be shown from the following considerations.

The Bragg law gives

$$\lambda = 2d_{(hkl)} \sin \theta$$

where

λ is the wave length of the incident electron beam,

d is the spacing between the successive (hkl) planes giving rise to the reflected spot, and

θ is the angle between the incident beam and the reflecting (hkl) planes.

The geometrical conditions corresponding to a given reflection are shown in Fig. 17. From the diagram it is seen that

$$\tan 2\theta = \frac{R}{L}$$

in which

2θ is the angle between the incident beam and the reflected beam,

R is the radius of the diffraction ring, and

L is the distance from the specimen to the photographic plate.

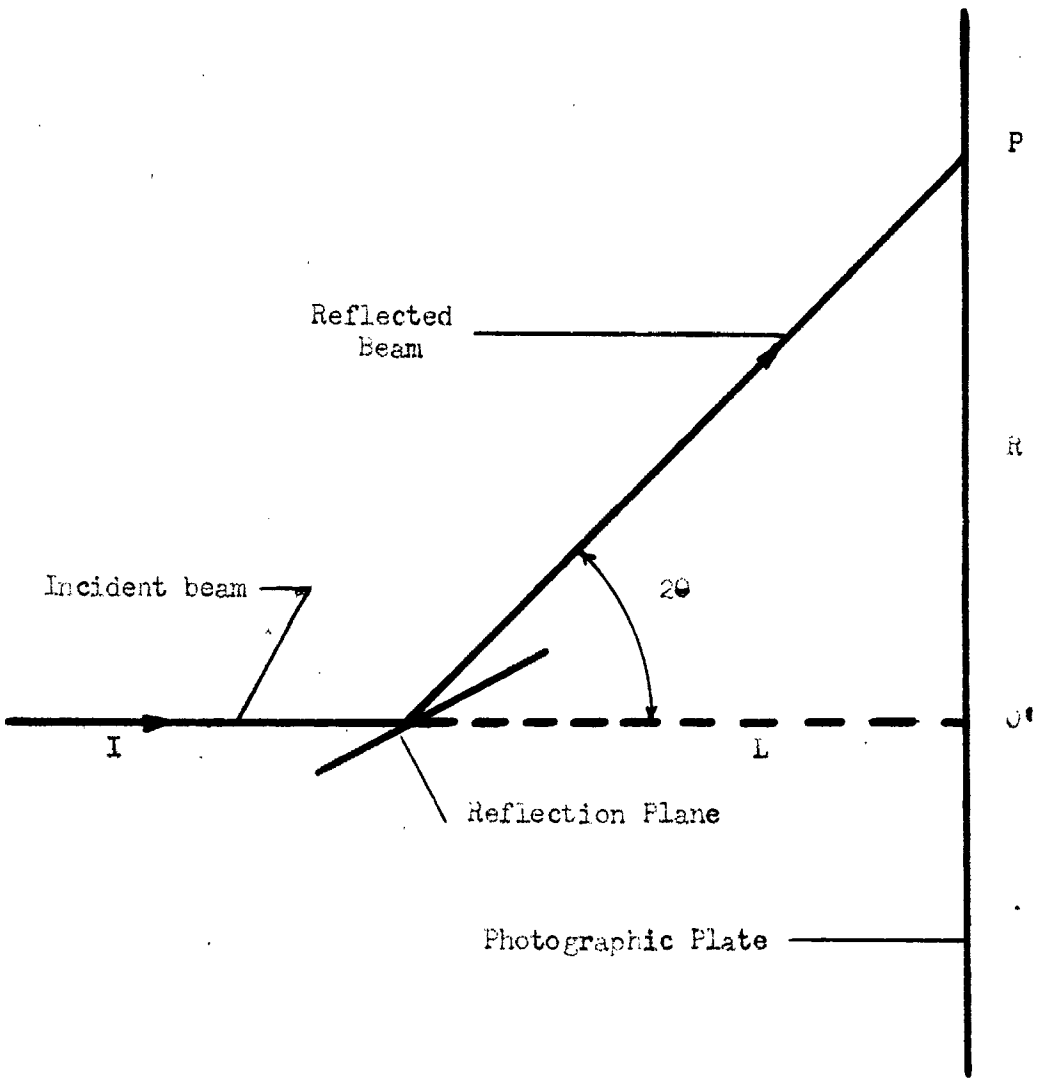

Fig. 17 - Showing Geometrical Relations Between the Incident and Reflected Beams of Electron Diffraction Photograph.

For the small angles covered in electron diffraction, the approximation can be made that

$$2\theta = \frac{R}{L}$$

Whence the Bragg equation can be written

$$\lambda = \frac{R}{L} d_{(hkl)}$$

or

$$d_{(hkl)} = \frac{\lambda L}{R}$$

Since the central spot in the diffraction photograph is usually obscure, it is of greater convenience to measure the ring diameters D. The above equation then becomes

$$d_{(hkl)} = \frac{2\lambda L}{D} \quad .$$

Calculation of the d-values from the observed ring diameters thus requires a knowledge of both L and λ.

In these experiments, the product λL was determined with the aid of photographs of zinc oxide (ZnO) used as a standard pattern. Zinc oxide in the form of a thin film was prepared by heating powdered Zn in air. Powdered zinc was placed in the fold of a piece of paper. A small porcelain crucible supported on a ring stand was heated with a gas-oxygen torch that had been adjusted to the hottest possible flame. When the crucible became incandescent the torch was removed and the powdered zinc placed in the crucible while the

crucible was still 'white' hot. The torch was immediately returned to its position under the crucible and a 200-mesh stainless-steel screen one centimeter on edge was held about ten centimeters above the crucible. Zinc oxide smoke collected on the screen. A film thickness that just left the screen visible through the zinc oxide film gave a good diffraction pattern.

The specimen of zinc oxide together with the molybdenum film that was previously floated off the rocksalt crystal, was mounted in a holder and placed in the specimen chamber of the diffraction instrument. The system was pumped to 10^{-3} millimeter of mercury pressure in the specimen box as indicated on the ion gage. Liquid nitrogen was then added to the cold trap. With the high voltage source adjusted to give 40 kilovolts at the electron gun, the gun filament was turned on and the beam focussed on the fluorescent shutter. When the molybdenum specimen was brought into position in the electron beam, the diffraction pattern could be observed on the fluorescent viewing screen at the back of the camera. The observed pattern, shown in Fig. 18, was photographed with an exposure time of twelve seconds. Using the same setting of L (the specimen-to-plate distance) and with the accelerating voltage held constant, the zinc oxide pattern in Fig. 19 was obtained. The exposure time was again 12 seconds.

Upon bringing the specimen into the electron beam by means of the specimen manipulator in the bottom plate of the chamber, the diffraction pattern could be observed on the shutter screen. When the sample was in position to give maximum intensity of the scattered

Fig. 18 - Electron Diffraction Pattern of Molybdenum Film Deposited on Natural Crystal of NaCl. Film Thickness Was Approximately 500 A.U.

Fig. 19 - Electron Diffraction Pattern of ZnO Film for Calibration of Diffraction Instrument.

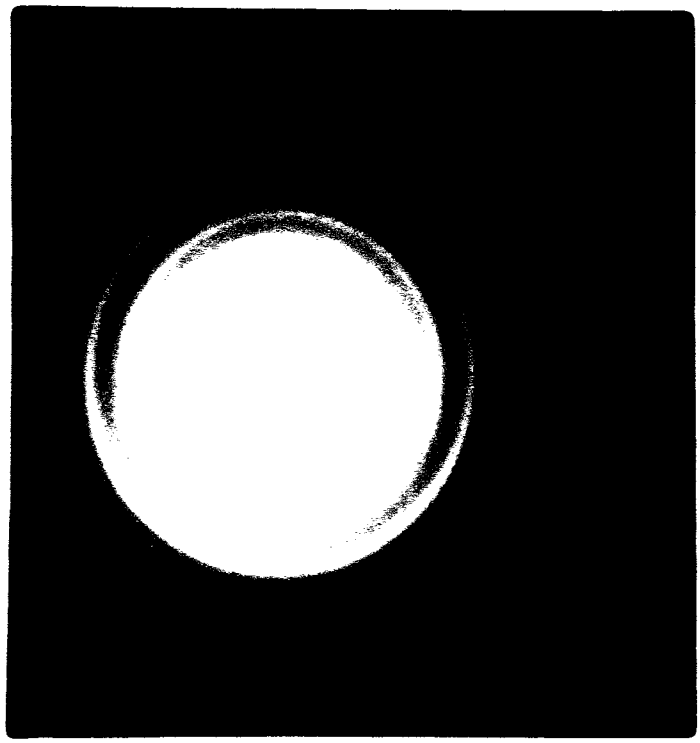

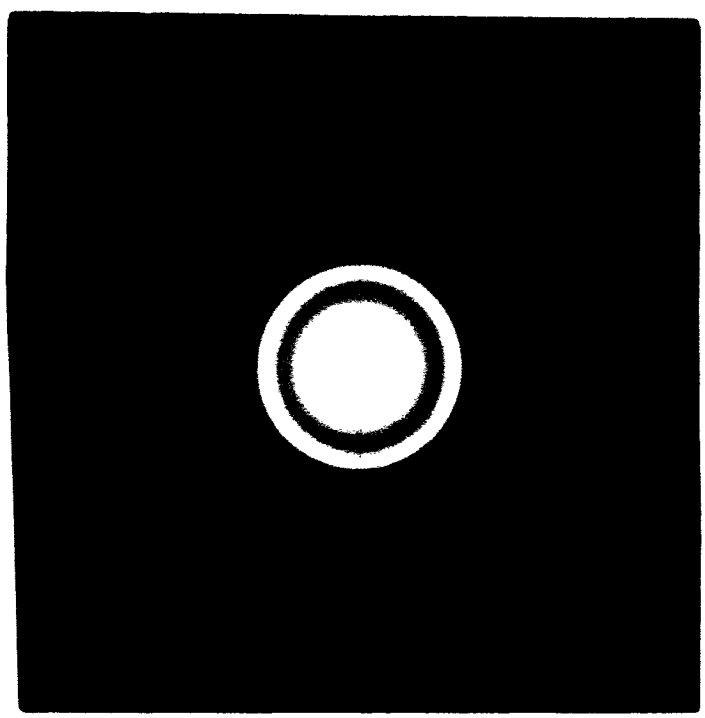

electrons, the pattern was photographed on thin glass photographic plates. Nominal size of the plates was 4 inches by 5 inches.

As has been mentioned earlier, samples that are too thick for penetration by the electron beam are studied by the reflection method. The molybdenum film that was deposited on the (100) face of the silver crystal was therefore examined by this method. The silver crystal was mounted in the specimen box of the diffraction instrument so that the (100) face of the crystal could be brought parallel to the electron beam. In this case, the beam strikes the crystal surface at nearly grazing incidence.

After the electron beam had been adjusted to 40 kilovolts and focussed on the shutter screen, the crystal face was brought into the beam for photographing. The best photographs were obtained with maximum contrast between the light and dark areas along the shadow edge of the pattern. Always a good pattern could be observed on the shutter screen, and the quality (contrast) and angular range of scattered electrons was better than appeared on the photographic plate. The pattern was photographed by retracting the shutter and exposing the photographic plate for 20-25 seconds. The crystal-to-film distance L was made the same as in the preceding experiments.

Thus far, emphasis has been on the preparation of specimens and the method of obtaining the electron diffraction photographs. It remains to analyze the diffraction patterns and to give quantitative definition of the results.

3. Calibration of Diffraction Instrument

In the equations given in the preceding section, the variables are the diffraction ring diameters D, the product $(2\lambda L)$, and the interplanar spacings d. If the product $(2\lambda L)$ is denoted by the letter K, then the above quantities are related by the equation

$$K = d_{(hkl)}D.$$

Now zinc oxide belongs to the crystallographic space group C6cm. That is, it has a hexagonal unit cell, with the constants a = 3.248 and c = 5.203. The d-spacing of the planes that give rise to each of the rings in the diffraction pattern of zinc oxide, Fig. 19, can be calculated from the expression

$$d_{(hkl)} = \frac{1}{\sqrt{\frac{4}{3}\left(\frac{h^2 + hk + k^2}{a^2}\right) + \frac{l^2}{c^2}}}$$

These values of d have been computed by Hanawalt (32) for the possible values of h, k, and l, and are listed in Table 3, column five. It is worth noting that with both λ and L fixed, the largest d-value corresponds to the smallest ring diameter, since there are no systematic absences in the diffraction pattern of zinc oxide, e.g. d_{100} = 2.81 A.U. Also for a given ring diameter D there is a fixed value of d. It follows that the value of K in the above equation can be found from the tabulated values of d and the measured ring diameters D.

Table 3 gives the observed values of the ring diameters for the electron diffraction pattern of ZnO shown in Fig. 19. The Miller indices of each of the diffraction rings are given in the first column of the table. Actual ring diameters were calculated by subtracting column two from column three. These values are tabulated in column four. The instrument calibration constant K was calculated using the product of columns four and five. With the value of K known from the zinc oxide pattern, the d-value of any reflection in the electron diffraction pattern of an unknown specimen may be calculated.

Measurements on the photographic plate were made by mounting a hair-line glass of an ordinary slide-rule on a horizontal screw attached to a viewing box. The screw was equipped to a micrometer scale, and an optical eyepiece was used for reading the scale. A piece of Scotch tape along two edges of the photographic plate held the plate in position on the viewing box while the measurements were being made.

Table 3. The Miller Indices (hkl) and the Observed Ring Diameters for the Electron Diffraction Pattern of Zinc Oxide Shown in Fig. 19.

Miller Index (hkl)	Scale Reading (cm) Left	Right	Ring Dia. D (cm)	Interplanar Spacing $d_{(hkl)}$	Calibration Constant K
(1)	(2)	(3)	(4)	(5)	(6)
100	2.138	4.528	2.390	2.81	6.72
002	2.040	4.621	2.581	2.61	6.74
101	1.964	4.698	2.734	2.46	6.73
102	1.576	5.089	3.513	1.91	6.71
110	1.267	5.390	4.123	1.61	6.64
103	1.064	5.600	4.536	1.47	6.67
112	0.896	5.772	4.876	1.38	6.73
203	0.274	6.391	6.117	1.09	6.67
				Mean:	6.70

III. EXPERIMENTAL RESULTS

A series of back-reflection Laue photographs is represented in Figs. 3, 7, 8 and 9. These patterns were taken to determine the orientation of the silver crystal and for cutting the crystal along a known crystallographic plane. Interzonal angles were measured from the photograph in Fig. 3, and these are recorded in Table 2 together with the Miller indices assigned to each zone. Table 4 gives the angles that were read on the circles of the goniometer when the X-ray beam was directed along an axis of crystal symmetry. All of the angles are given with respect to a fixed coordinate system in the crystal. The angle θ measures the rotation of the specimen about the X-ray beam or the axis of x, ϕ gives the angular rotation about an intermediate axis η, and ψ is the angular coordinate of the reference line on the crystal or rotation about the cylinder axis of the crystal; rotation of the goniometer about its vertical axis is designated by ψ'.

Angles θ, ϕ, and ψ are referred to as Euler angles. Counter clockwise rotation when looking along an axis in the direction of the origin was taken as the positive sense of all angles. The coordinate system used to describe the orientation of the crystal is given in Appendix A.

In Fig. 7 the X-ray beam is parallel to a four-fold axis of symmetry. A check on the exact orientation of the unit cell is obtained from Figs. 8 and 9. Figure 8 was taken after rotating the goniometer about the Z-axis through an angle of +90° from its position

in Fig. 7. The pattern in Fig. 9, showing three-fold symmetry, was obtained after rotating the specimen through an angle of 54°44' from its position in Fig. 7. Thus, the photographs in Figs. 7, 8, and 9 were taken with the X-ray beam parallel to the four-fold, two-fold, and three-fold axes of symmetry of the crystal, respectively.

Table 4. Angles Observed on Goniometer When X-Ray Beam was Parallel to the Axis of Symmetry Shown, for f.c.c. Silver Crystal

Symmetry Axis	Angles on Goniometer θ	ϕ	ψ	ψ'	Ref. Fig.
4-fold	-13.7°	23.4°	-42.5°	0°	7
3-fold	-13.7°	23.4°	-42.5°	54.6°	8
2-fold	-13.7°	23.4°	-42.5°	90°	9

With the orientation of the crystal determined relative to a fixed reference frame, the specimen was mounted in the Index Center of a precision milling machine and cut along a (100) face of the crystal. A second specimen was prepared by cutting the crystal parallel to a (110) surface. Figure 11 shows the back-reflection photograph of the crystal when the X-ray beam was normal to the (100) plane. This photograph was taken immediately after cutting the crystal and before any further treatment of the specimen.

Continuous rings indicate the random orientation of the silver crystallites, to the depth of penetration of the X-rays.

After mechanically polishing the (110) surface of the silver crystal on metallographic emery papers and electropolishing in a cyanide solution, the X-ray photograph in Fig. 12 was obtained. Besides showing the single crystal structure of the face that had been cut and polished, Fig. 12 establishes the validity of the transformation matrix developed in Appendix A. This matrix was developed in order to determine the angles α, β, and γ to be set on the Index Center for cutting the desired crystal face. These angles, listed in Table 5, fix the orientation of the Index Center and the crystal such that the axis of the cutting tool is parallel to the given crystallographic axis of symmetry.

The single crystal structure of the polished (110) face is shown on an atomic scale in the electron diffraction pattern in Fig. 20. Elongation of the spots in one direction can be attributed to the limited depth of penetration of the incident electrons. A thin film of molybdenum was deposited on a (100) face of silver similar to the one that gave the diffraction pattern in Fig. 20.

The molybdenum films were evaporated in the vacuum apparatus shown schematically in Fig. 14. A film was deposited on the silver crystal at a temperature of 350 degrees centigrade. When the crystal had cooled to room temperature, it was removed from the evaporation tube and immediately afterwards the surface was studied by electron diffraction. The molybdenum film deposited on a natural crystal of

Fig. 20 - Electron Diffraction Pattern of Silver Crystal After Electropolishing. Beam Incident Along (110) Surface.

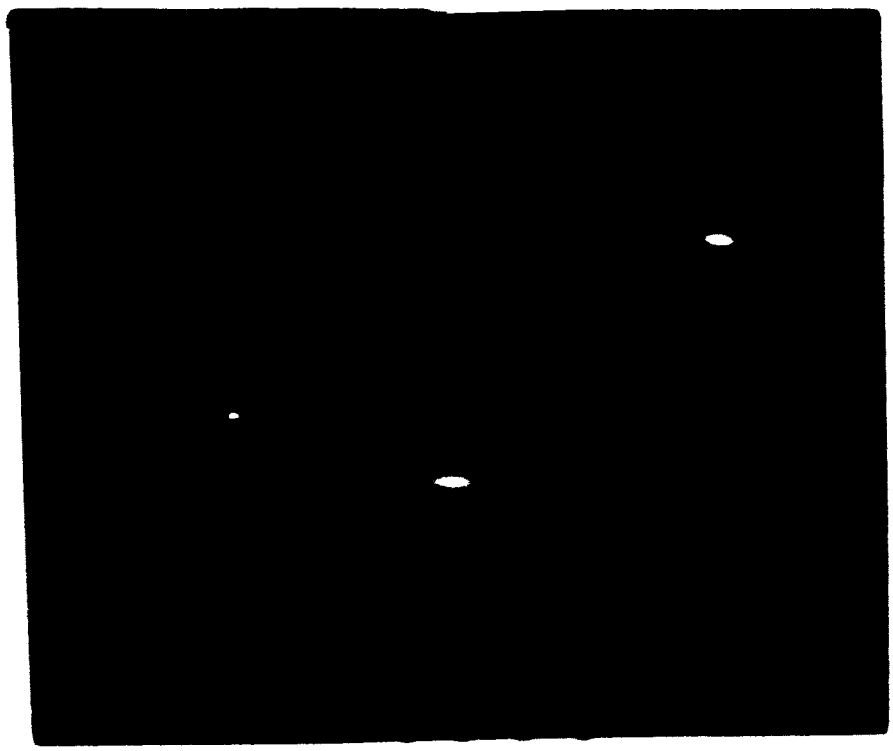

Table 5. Angles Set on Index Center of Milling Machine When Axis of Cutting Tool Is Parallel to a Given Crystallographic Axis of Crystal.

Symmetry Axis of Cutting Tool	Angles Set on Index Center		
	α	β	γ
4-fold	28.7°	26.9°	-73.9°
3-fold	83.3°	26.9°	-73.9°
2-fold	-61.3°	26.9°	-73.9°

Table 6. Data Obtained from Measurements of Electron Diffraction Ring Pattern of Fig. 16. Molybdenum Evaporated onto Cleaved Surface of Rocksalt.

Scale Reading (cm) Left	Right	Ring Dia. D	Interplanar Spacing d*	Miller Index (hkl)	Lattice Constant a	Relative Intensity I_1/I_o
(1)	(2)	(3)	(4)	(5)	(6)	(7)
4.506	7.495	2.989	2.24	101	3.17	1.0
3.886	8.118	4.232	1.58	200	3.16	0.5
3.421	8.592	5.171	1.30	112	3.17	0.8
3.006	8.993	5.987	1.12	220	3.16	0.2
2.656	9.357	6.701	1.00	103	3.16	0.4

*d = K/D, K = 6.70 from Table 3.

sodium chloride was caught on a piece of 200-mesh stainless steel screen and investigated by the electron beam. By means of a multiple-beam interferometer, the film deposited on the rocksalt crystal was found to be approximately 500 Angstrom units in thickness.

The layer deposited on rocksalt was obtained by evaporation from a 0.005 inch molybdenum filament. The diffraction pattern in Fig. 18 shows that this film has the body centered cubic structure of molybdenum with lattice constant of 3.16 Angstrom units, compared with the value of 3.144 Angstrom units obtained by X-rays. Continuous rings are due to the random orientation of small molybdenum crystals. Table 6 gives the data obtained from measuring the diameters of the diffraction rings of the molybdenum pattern in Fig. 18. Values of the interplanar spacing d were calculated from the relations developed under "Calibration of Diffraction Instrument". The lattice constant "a" was found from the expression

$$a = d\sqrt{h^2 + k^2 + l^2}$$

where (h,k,l) are the Miller indices of the observed reflection and "a" is the lattice constant of the cubic unit cell of molybdenum. Relative intensities of the diffraction rings are given in the last column of Table 6.

It was estimated that the metallic film formed by evaporation of molybdenum on the (100) face of silver was 100-150 Angstrom units in thickness. The thickness of the film was not determined by the

interferometric method but was estimated from the geometry of the experimental set-up shown in Fig. 15. The separation of the filament and the (100) surface of the silver crystal was about double that of the filament and rocksalt crystal on which a film 500 Angstrom units thick was deposited. Application of the inverse square law would thus indicate a film thickness of 125 Angstrom units. However, as the filament was not a point source of radiation, the inverse square law gives only an approximation to the thickness of the molybdenum film evaporated onto the silver crystal. The filament current and the period of evaporation were the same in both cases. Figure 21 shows the diffraction pattern of this layer obtained by 'reflection' of 40 kilovolt electrons from the surface of the crystal. The film was identified as molybdenum by superimposing the photographic plate of Fig. 18 over the pattern in Fig. 21. The diffraction ring systems coincide on the two photographs.

Figure 22 shows a reflection photograph that was taken of a freshly cleaved and polished crystal of rocksalt. The electron diffraction pattern of a collodion film is shown in the picture of Fig. 23. Collodion, like glass, has an amorphous structure in which there is no regular arrangement of atoms.

Fig. 21 - Reflection Pattern From Molybdenum Film Deposited on (100) of Silver Crystal. Thickness of Film 100-150 A.U.

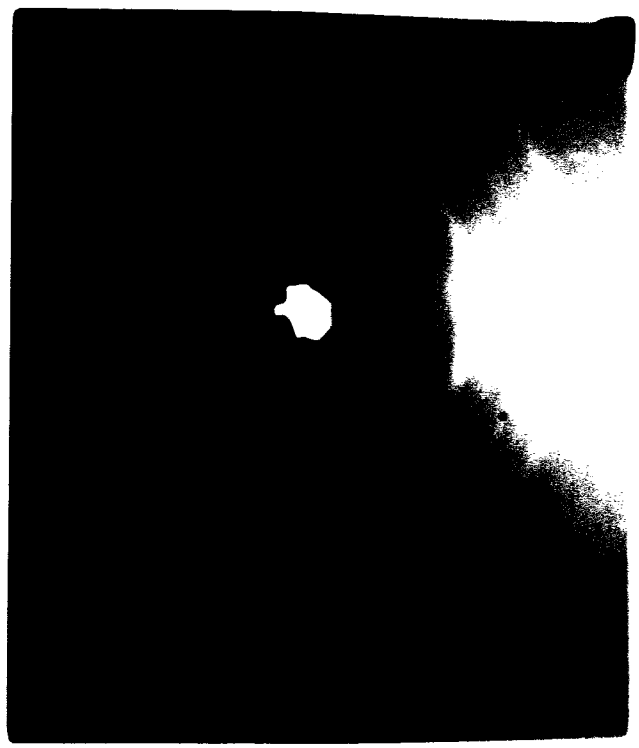

Fig. 22 - Electron Diffraction Pattern of Freshly Cleaved and Polished Surface of Natural Sodium Chloride Crystal.

Fig. 23 - Electron Diffraction Pattern of Collodion Film Obtained With 40kv Electrons.

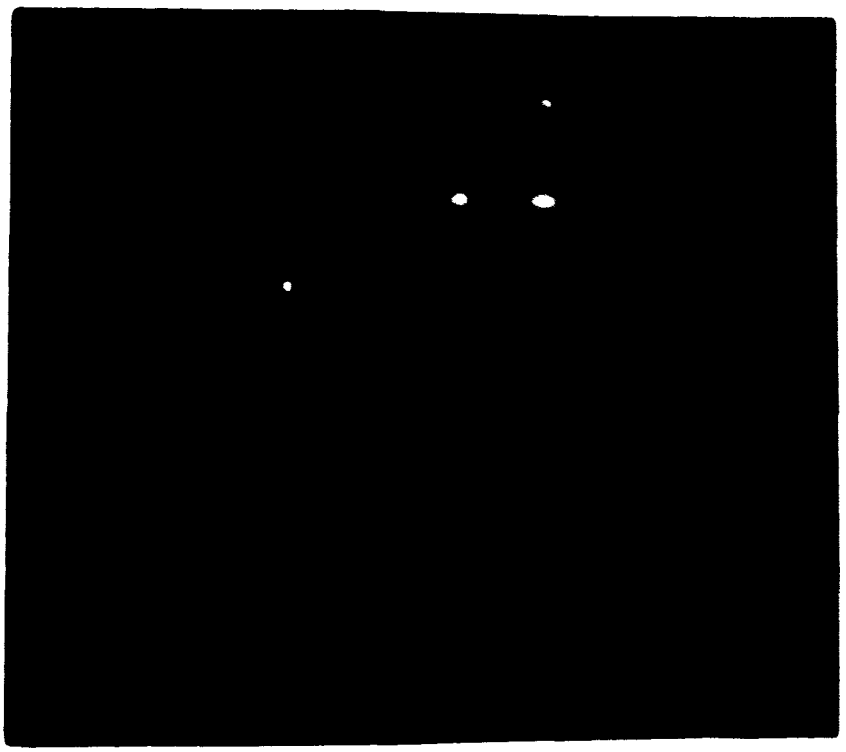

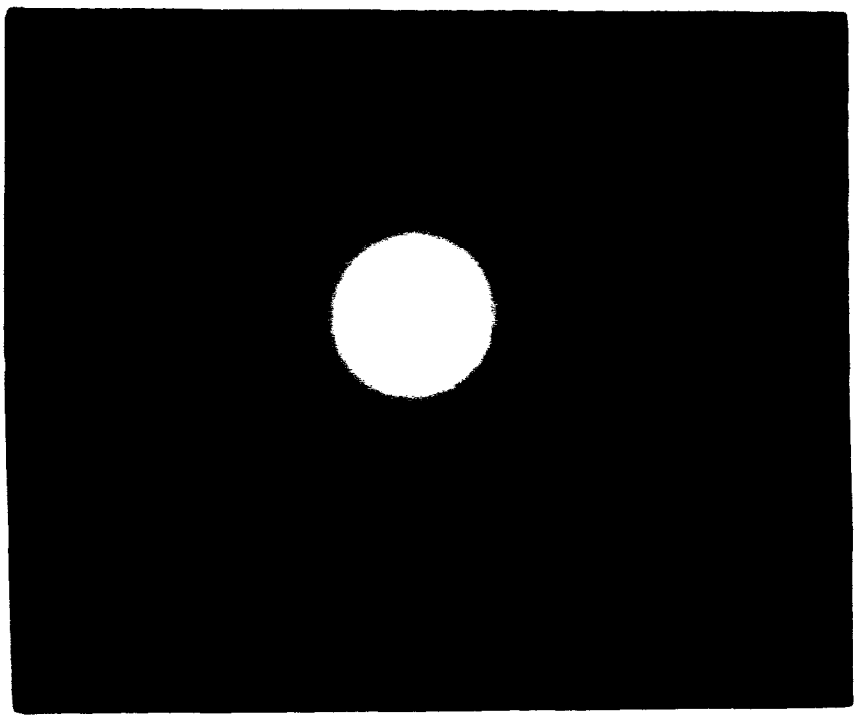

IV. SUMMARY AND CONCLUSION

In summarizing it can be said that after the orientation of the single crystal specimen of silver had been determined by the back-reflection Laue method, the specimen was cut along a known crystallographic plane, using apparatus that was available in the machine shop. The intermediate step between orienting and cutting the single crystal required the development of a transformation matrix. This matrix related the angles on the circles of the Index Center of a precision milling machine with the known orientation angles observed on the X-ray goniometer. The transformation matrix was developed from the classical theory of rotation of rigid bodies, making use of the Euler angles as the three independent coordinates of the rotations.

A single crystal of silver in the form of a rod 5/8 inch in diameter was cut parallel to the (100) and the (110) faces using the above method. The angles α, β, and γ that determine the orientation of the crystal in the Index Center of the milling machine were calculated from the known angles θ, ϕ, and ψ. These angles were related through the transformation matrix T developed in Appendix A. Back-reflection X-ray photographs that were taken after cutting and electrolytically polishing the crystal surfaces confirm the validity of the method.

Having obtained a crystal face of known configuration, experiments were undertaken to study the structure of thin molybdenum films evaporated onto the known surface. Molybdenum was evaporated

from a 0.005 inch filament in a kinetic vacuum system and then condensed from the gas phase. First, the freshly cleaved cube face of a natural sodium chloride crystal was used as base for the condensed metal. Later, the metal was condensed on the heat-treated and polished (100) face of a silver crystal. Metallic films, 150 and 500 Angstrom units in thickness, were prepared in this manner. In both instances the deposited film showed the lattice structure of metallic molybdenum when examined by electron diffraction. The ring patterns indicate the completely random orientation of the crystallites in the deposited layer.

While thin deposits of some metals on the cleaved surface of rocksalt have been observed (20) to take up a preferred orientation when the temperature during evaporation is above a certain critical value, the actual thickness of the deposited layer is not known. It seems likely that films several atomic layers in thickness would show an orientation that is related to the atomic arrangement at the interface with the substrate, but that as the film becomes thicker the deposit would take up a random orientation. This may explain the absence of oriented overgrowth in the molybdenum film, 500 Angstrom units in thickness, deposited on the (100) face of rocksalt.

Relative to the molybdenum film deposited on the (100) face of a silver crystal, close examination of Fig. 21 shows several spots that do not lie on the diffraction rings of the molybdenum pattern. One can only conclude that these are reflections from the silver crystal substrate, and hence that the electrons in the incident beam must have

penetrated the molybdenum film 100-150 Angstrom units in thickness. This result is in agreement with experiments reported by other workers (6) who have observed depths of penetration of more than 200 Angstrom units in metallic films.

Although the pattern in Fig. 21 does not show a preferred orientation in the deposited film, it may be that at some critical temperature the crystallites of body centered cubic molybdenum would grow with their axes oriented in a definite manner relative to the underlying face centered cubic silver crystal. It may be too that when depositing a very thin film a few atom layers in thickness on a dissimilar metal, the evaporated metal could be induced to take up the crystal structure of the base metal as well. There is also a need for further study on the physical properties including resistivity, surface reactions such as corrosion, and optical measurements on thin films of one metal deposited on a different metal.

V. LITERATURE CITED

1. De Broglie, L. Phil. Mag. 47, 446 (1924).
2. Davisson, C. J. and L. H. Germer. Phys. Rev. 30, 705 (1927).
3. Thomson, G. P. Proc. Roy. Soc. Lond. A 117, 600 (1928).
4. Nishikawa, S. and S. Kikuchi. Nature 122, 726 (1928).
5. Finch, G. I. and H. Wilman. Ergeb. exakt. Naturw. 16, 353 (1937).
6. Cochrane, W. Proc. Phys. Soc. Lond. 48, 723 (1936).
7. Shirai, S. Proc. Phys.-Math. Soc. Japan 19, 937 (1937).
8. Thomson, G. P. Proc. Roy. Soc. Lond. A 128, 649 (1930).
9. Bragg, W. L. Proc. Camb. Phil. Soc. 17, 43 (1913).
10. Kirchner, F. and H. Raether. Physik. Zeits. 30, 510 (1932).
11. Bragg, W. L. Nature 124, 125 (1929).
12. French, R. C. Proc. Roy. Soc. Lond. A 140, 637 (1933).
13. Kirchner, F. Trans. Faraday Soc. 31, 1114 (1935).
14. Boumann, J. Selected Topics in X-ray Crystallography, Interscience Publishers, N.Y., 1951.
15. Gwathmey, A. T. The Preparation of Single Crystals for the Study of Surface Reactions. In Pittsburgh International Conference on Surface Reactions. p. 66-70. Corrosion Pub. Co., Pittsburgh, Pa., 1948.
16. Lassen, H. and L. Brück. Ann. d. Physik 22, 65 (1935).
17. Dixit, K. R. Phil. Mag., 16, 1049 (1933).
18. Rhodin, T. N. Trans. AIME, 185, 371 (1949).
19. Schulz, L. G. Acta Cryst. 5, 130 (1952).

20. Shirai, S. Proc. Phys.-Math. Soc. Japan 23, 12 (1941).

21. _____. Proc. Phys.-Math. Soc. Japan 23, 914 (1941).

22. Gwathmey, A. T. and A. F. Benton. J. Phys. Chem. 44, 35 (1940).

23. Greninger, A. B. Zeits. f. Krist. 91, 424 (1935).

24. Barrett, C. S. Structure of Metals, McGraw-Hill Book Co., Inc., N. Y., 1952.

25. Gilbertson, L. I., and D. W. Fortner. Trans. Electrochem. Soc. 81, 199 (1942).

26. Jaquet, P. A. Metal Finishing 47, 48-54 (1949).

27. Epelboin, I., and C. Chalin. Compte Rendus 226, 324-6 (1948).

28. Strong, J. Procedures in Experimental Physics, Prentice-Hall, Inc., N. Y., 1946.

29. Bearinger, W. V. Ph.D. Thesis, Iowa State College, 1950.

30. RCA Electron Microscope Instruction Manual. I. B. 39008-2, Camden, N. J., 1946.

31. Hanawalt, J. D., H. W. Rinn, and L. K. Frevel. Ind. and Eng. Chem. 10, 457 (1938).

32. Metals Handbook, 1948 Edition. The Am. Soc. for Metals, Cleveland, Ohio.

33. International Critical Tables 6, McGraw-Hill Book Co., Inc., N. Y., 1929.

34. Corben, H. C. and P. Stehle. Classical Mechanics, John Wiley and Sons, N. Y., 1950.

VI. ACKNOWLEDGEMENTS

Grateful acknowledgement is made for assistance in preparing this thesis to Dr. W. B. Boast for his interest and enccuragement throughout the investigation; Dr. D. W. Stebbins for assistance in the experimental work; Dr. L. S. Bartell whose suggestions and assistance materially aided in the completion of this work; and to Dr. R. E. Rundle for helpful suggestions and for use of the facilities of the X-ray laboratory. The author wishes also to express appreciation to members of the Glass Shop and the College Instrument Shop for assistance in the experimental work, and in particular to Mr. Richard Brown for help in cutting the metal single crystals.

Thanks are due the Office of Ordnance Research whose financial assistance made this work possible.

VII. APPENDICES

APPENDIX A

Method of Orientation and Cutting of Single Crystals

The orientation of a Cartesian set of axes relative to another set with a common origin is specified by giving the direction cosines of the one set, say the primed set in Fig. A, relative to the other unprimed set. This method of specifying the orientation of the primed set relative to the unprimed axes requires a set of nine direction cosines. If the primed axes are taken as fixed in the body, these nine direction cosines degenerate into a set of three independent coordinates. A number of such sets of independent variables have been described in the literature but the most common and useful are the Euler angles (34). These angles can be represented most easily on the surface of a sphere, whose center is at the common origin of all of the orthogonal coordinate systems. In the geometrical construction, radial lines or axes appear as points on the surface of the sphere; and plane angles between pairs of central axes appear as great circle arcs in the planes of the great circles defined by the pairs of axes.

The transformation from a given Cartesian coordinate system to another can then be carried out by three successive rotations taken in a specific sequence. The Euler angles are defined as the three successive angles of rotation, and in terms of the motions of the goniometer, they are Θ, ϕ and ψ . The Euler augles Θ, ϕ, and ψ

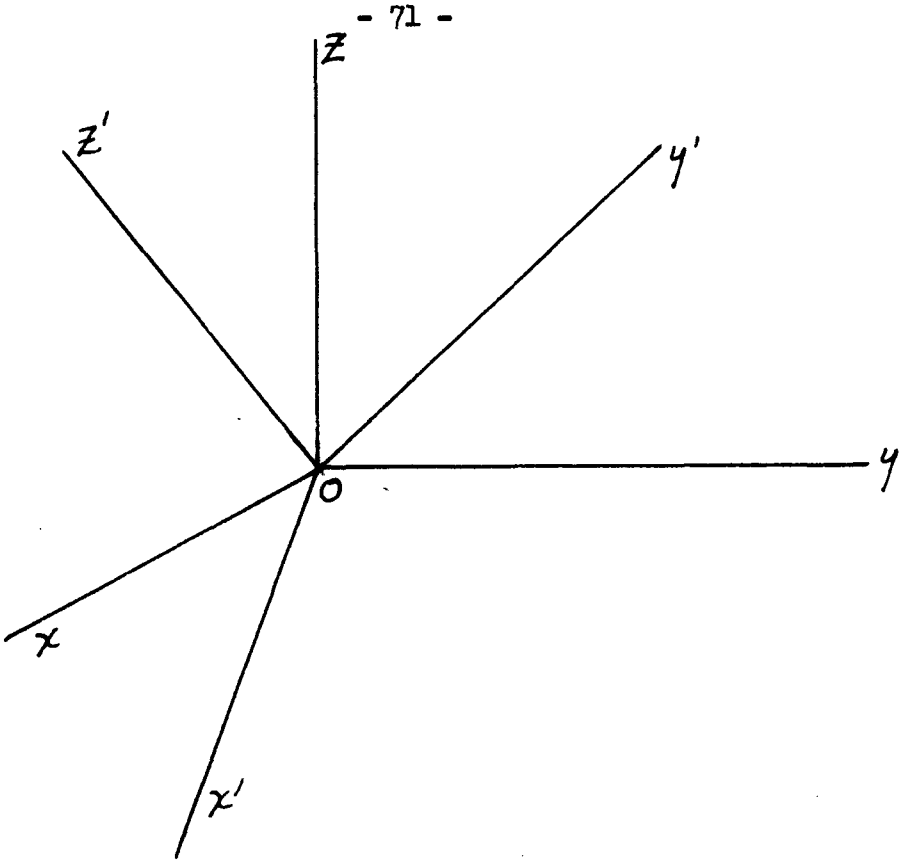

Fig. A - Cartesian Axes xyz Represent the Reference Frame. x'y'z' Are Fixed in the Crystal.

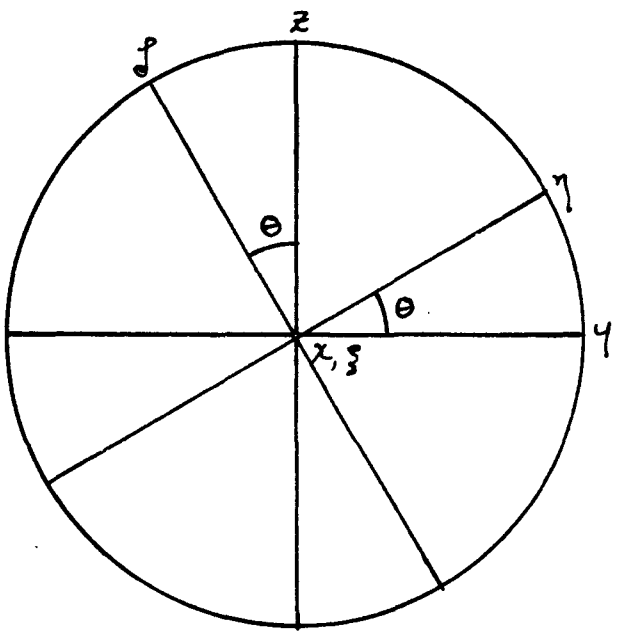

Fig. B - Orientation of Axes After Initial Rotation.

completely specify the orientation of the x'y'z' system relative to the xyz and can therefore be used as the three independent coordinates.

The matrix of the transformation from xyz to x'y'z' can be written as the triple product of the matrices arising from the successive single-axis rotations.

The initial rotation about x is shown in Fig. B and the corresponding transformation from x,y,z, to ξ, η , ζ can be written in the form

$$\begin{bmatrix} \xi \\ \eta \\ \zeta \end{bmatrix} = \overset{W}{\begin{bmatrix} 1 & 0 & 0 \\ 0 & \cos\theta & \sin\theta \\ 0 & -\sin\theta & \cos\theta \end{bmatrix}} \times \begin{bmatrix} x \\ y \\ z \end{bmatrix}$$

The transformation from ξ, η, ζ to ξ', η', ζ' is shown with the initial rotation on the diagram in Fig. C and is given in matrix form by

$$\begin{bmatrix} \xi' \\ \eta' \\ \zeta' \end{bmatrix} = \overset{V}{\begin{bmatrix} \cos\phi & 0 & -\sin\phi \\ 0 & 1 & 0 \\ \sin\phi & 0 & \cos\phi \end{bmatrix}} \times \begin{bmatrix} \xi \\ \eta \\ \zeta \end{bmatrix}$$

The last rotation through the angle ψ has the matrix

$$\begin{bmatrix} x' \\ y' \\ z' \end{bmatrix} = \overset{U}{\begin{bmatrix} \cos\psi & \sin\psi & 0 \\ -\sin\psi & \cos\psi & 0 \\ 0 & 0 & 1 \end{bmatrix}} \times \begin{bmatrix} \xi' \\ \eta' \\ \zeta' \end{bmatrix}$$

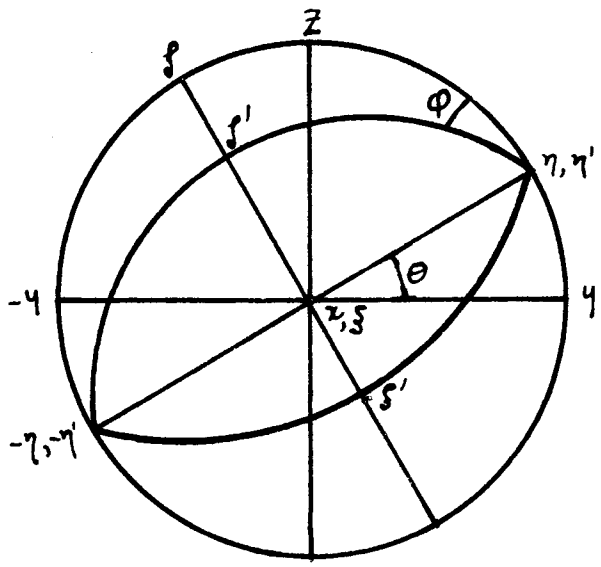

Fig. C - Orientation of Axes After Intermediate Rotation About the η-Axis Through An Angle ϕ.

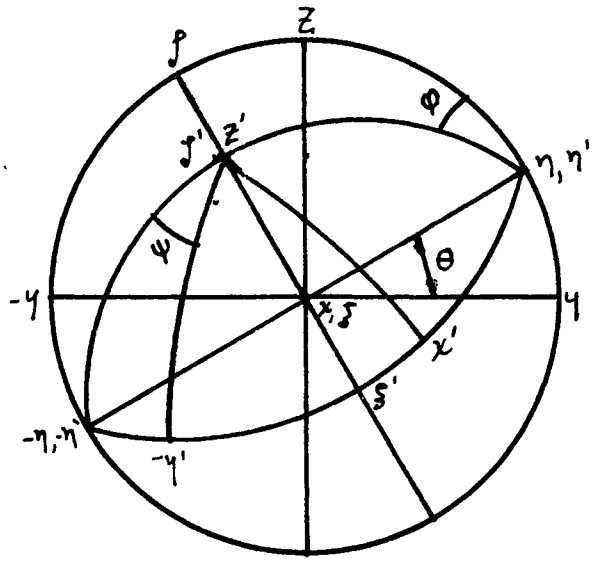

Fig. D - Orientation of Axes After Final Rotation About the ζ'-Axis Through An Angle ψ.

The product matrix which transforms xyz into x'y'z' can then be written[a]

$$\begin{bmatrix} x' \\ y' \\ z' \end{bmatrix} = \overset{T}{\begin{bmatrix} C\psi C\phi & C\theta S\psi + S\theta C\psi S\phi & S\psi S\theta - C\psi C\theta S\phi \\ -C\phi S\psi & C\theta C\psi - S\theta S\phi S\psi & S\theta C\psi + C\theta S\phi S\psi \\ S\phi & -S\theta C\phi & C\theta C\phi \end{bmatrix}} \times \begin{bmatrix} x \\ y \\ z \end{bmatrix}$$

where

$$T = UVW.$$

The order of the multiplications is unimportant since (UV)W = U(VW). Figure D shows the orientation of the primed axes, x', y', z' after the three single-axis rotations.

In a similar manner the transformation matrices corresponding to the rotations of the Index Center were derived in terms of the Euler angles α, β, and γ, shown on the surface of the sphere in Fig. E.

The first rotation through the angle α gives

$$\begin{bmatrix} \xi_i \\ \eta_i \\ \zeta_i \end{bmatrix} = \overset{W_i}{\begin{bmatrix} \cos\alpha & \sin\alpha & 0 \\ -\sin\alpha & \cos\alpha & 0 \\ 0 & 0 & 1 \end{bmatrix}} \times \begin{bmatrix} x_i \\ y_i \\ z_i \end{bmatrix}$$

Rotation about η_i through the angle β transforms ξ_i, η_i, ζ_i into ξ'_i, η'_i, ζ'_i. The matrix of the transformation is V_i:

---

[a] The trigonometric functions of sine and cosine have been abbreviated by "S" and "C", respectively. Thus, cos θ is written Cθ, and sin θ as Sθ.

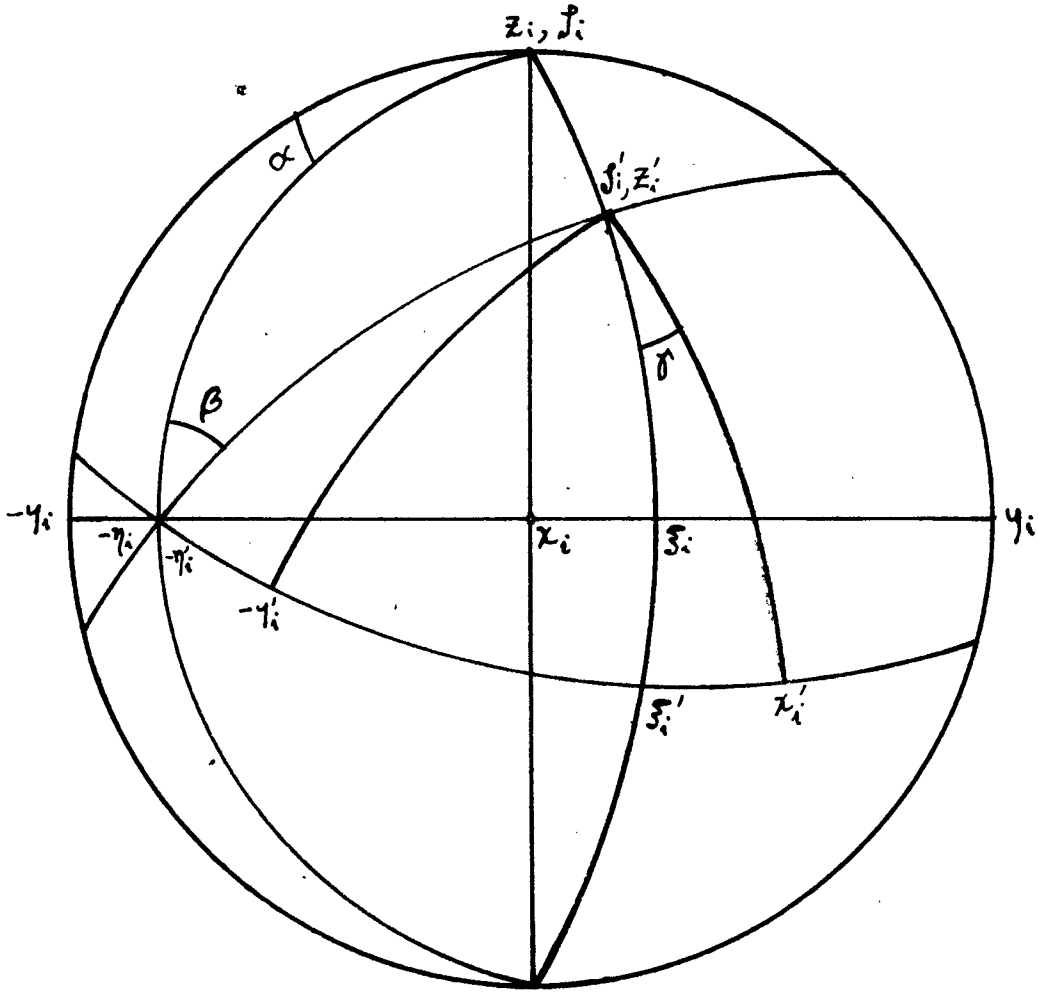

Fig. E - Orientation of Axes After Rotation Through The Angles α, β, and γ On The Index Center.

$$\begin{bmatrix} \xi_i' \\ \eta_i' \\ \zeta_i' \end{bmatrix} = \overset{V_i}{\begin{bmatrix} \cos\beta & 0 & -\sin\beta \\ 0 & 1 & 0 \\ \sin\beta & 0 & \cos\beta \end{bmatrix}} \times \begin{bmatrix} \xi_i \\ \eta_i \\ \zeta_i \end{bmatrix}$$

And the final rotation into x_i', y_i', z_i' is given by the matrix U_i

$$\begin{bmatrix} x' \\ y' \\ z' \end{bmatrix} = \overset{U_i}{\begin{bmatrix} \cos\gamma & \sin\gamma & 0 \\ -\sin\gamma & \cos\gamma & 0 \\ 0 & 0 & 1 \end{bmatrix}} \times \begin{bmatrix} \xi'_i \\ \eta'_i \\ \zeta'_i \end{bmatrix}$$

The complete transformation matrix is

$$T_i = U_i\, V_i\, W_i$$

$$= \begin{bmatrix} C\alpha C\beta C\gamma - S\alpha S\gamma & S\alpha C\beta C\gamma + C\alpha S\gamma & -S\beta C\gamma \\ -C\alpha C\beta S\gamma - S\alpha C\gamma & -S\alpha C\beta S\gamma + C\alpha C\gamma & S\beta S\gamma \\ C\alpha S\beta & S\alpha S\beta & C\beta \end{bmatrix}$$

and

$$\begin{bmatrix} x_i' \\ y_i' \\ z_i' \end{bmatrix} = \begin{bmatrix} \\ T_i \\ \\ \end{bmatrix} \times \begin{bmatrix} x_i \\ y_i \\ z_i \end{bmatrix} .$$

It may be noted that the sum of the squares of the direction cosine functions in any row or column of T_i adds to unity.

To find the values of α, β, and γ, the angles to be set on the Index Center, in terms of the known goniometer angles Θ, ϕ, and ψ, we have only to equate the matrices T and T_1; then to cut the crystal along a (100) face for which $\Theta = -13.7°$, $\phi = 23.4°$, $\psi = -42.5°$; and if $T_1 = T$ it follows that

$$\cos \beta = \cos \Theta \cos \phi = .8915$$

$$\sin \alpha \sin \beta = -\sin \Theta \cos \phi$$

$$\cos \alpha \sin \beta = \sin \phi$$

$$\tan \alpha = .5470$$

$$\sin \gamma = -.9611$$

The solution of these equations gives

$$\alpha = 28.7°$$

$$\beta = 26.9°$$

$$\gamma = -73.9° \quad .$$

With the circles of the Index Center set at the values of α, β, and γ just determined, the axis of the saw is normal to the (100) face of the crystal.

The correct orientation for cutting the crystal along a (110) plane is determined by first rotating the goniometer through an angle of 90° about the Z-axis. This introduces a fourth transformation W'. When the matrix of this fourth transformation is combined with the three preceding matrices, U, V, and W, the transformation matrix T' for the (110) direction is obtained. Thus

$$T' = TW' \quad .$$

where

$$\begin{bmatrix} W' \end{bmatrix} = \begin{bmatrix} 0 & 1 & 0 \\ -1 & 0 & 0 \\ 0 & 0 & 1 \end{bmatrix}$$

If the matrix T_i is now put equal to T', the angles to be set on the Index Center are found to be

$$\alpha = -61.3°$$

$$\beta = 26.9°$$

$$\gamma = -73.9°$$

The transformation matrix for cutting the crystal along a (111) face is obtained by combining the T matrix with a rotation of 54°44' about the Z-axis. For this condition

$$T'' = TW''$$

where

$$\begin{bmatrix} W'' \end{bmatrix} = \begin{bmatrix} 0.5775 & 0.8164 & 0 \\ -0.8164 & 0.5775 & 0 \\ 0 & 0 & 1 \end{bmatrix}$$

in which

$$\cos (54°44') = 0.5775$$

$$\sin (54°44') = 0.8164 \quad .$$

The corresponding angles on the Index Center can be determined by putting

$$T_i = T''$$

then

$$\alpha = 83.9°$$

$$\beta = 26.9°$$

$$\gamma = -73.9°$$

It should be mentioned that in all of the above rotations, the angles θ and α are with respect to the x, y, z system of coordinates or the inertial frame of reference.

APPENDIX B

Calculation of Molybdenum Filaments

The dimensions of the molybdenum filaments were calculated assuming that the ohmic power (I^2R) supplied to the filament was dissipated by radiation from the filament. All of the physical constants used were obtained from references 32 and 33.

The power loss by radiation is given by the Stefan-Boltzmann law as

$$M = \varepsilon \sigma T^4 \text{ watts per square meter}$$

where

$\varepsilon = 0.29$, the emissivity coefficient

$\sigma = 5.672 \times 10^{-8}$ watts per sq. meter per $°K^4$, Boltzmann constant

$T = 2898$ °K, the melting point of molybdenum.

Upon substituting these values, the power loss by radiation from the heated filament is

$$M = 0.29 \times 5.672 \times 10^{-8} \times (2,898)^4$$

$$= 116.0 \times 10^4 \text{ watts per square meter.}$$

The current required to raise the temperature of the filament to the melting point is determined from the following relations:

$$I^2 = \frac{Q}{R} = \frac{QA_c}{\rho L} = \frac{\pi D^2 Q}{4\rho L}$$

$$= \frac{\pi^2 D^3 Q}{4\pi D L \rho} = \frac{Q}{A_s} \times \frac{\pi^2 D^3}{4\rho}$$

$$= \frac{M \pi^2}{4\rho} \times D^3 .$$

Hence $I = K \ D^{3/2}$

where

$$K = \frac{\pi}{2} \sqrt{\frac{M}{\rho}}$$

and D = diameter of filament in meters

$M = \frac{Q}{A_s}$, the power loss by radiation in watts per sq. meter.

ρ = resistivity of molybdenum in ohm-meters.

I = filament current in amperes

A_s = surface area of filament in square meters

Q = ohmic power supplied to filament in watts

A_c = cross-sectional area of filament in sq. meters

L = length of filament in meters

R = resistance of filament in ohms

E = potential applied to filament in volts.

The resistivity ρ of molybdenum at the melting point temperature $t = 2625°C$ is calculated from the series expansion, in which $t' = 0°C$:

$$\rho_t = \rho_{t'} \left[1 + \alpha(t - t') \times 10^{-3} + \beta(t - t') \times 10^{-6}\right]$$

$$= 5.14 \times 10^{-6} \left[1 + 4.791 \times 2625 \times 10^{-3} + .346 \times (2625)^2 \times 10^{-6}\right]$$

$$= 5.14 \times 10^{-6} \times 15.95$$

$$= 82.0 \times 10^{-8} \text{ ohm-meters.}$$

Using the values of M and ρ obtained above, the constant K is determined from the equation

$$K = \frac{\pi}{2} \sqrt{\frac{M}{\rho}}$$

$$= \frac{\pi}{2} \sqrt{\frac{116.0 \times 10^4}{82 \times 10^{-8}}}$$

$$= 1.87 \times 10^6$$

Whence for a 0.005 inch filament the current required for evaporation is

$$I = KD^{3/2}$$

$$= 1.87 \times 10^6 \, (1.27 \times 10^{-4})^{3/2}$$

$$= 2.7 \text{ amperes.}$$

The filament voltage corresponding to this value of current is

$$E = RI$$

$$= \frac{4\rho L}{\pi D^2} \quad \frac{\pi}{2} \sqrt{\frac{M}{\rho}} \; D^{3/2}$$

$$= 2 \sqrt{\frac{M\rho}{D}} \; L \text{ volts}$$

From which

$$\frac{E}{L} = 2 \times \sqrt{\frac{116.0 \times 10^{4} \times 82.0 \times 10^{-8}}{1.27 \times 10^{-4}}}$$

$$= 173.0 \text{ volts per meter.}$$

Hence, for a filament length of 6.5 centimeters the required voltage is approximately 11 volts. This filament voltage and the current of 2.7 amperes are conveniently obtained from a 115-volt, 5-ampere Variac.